รายงานวิจัยฉบับสมบูรณ์

โครงการ กรดอะมิสำคัญในโครงสร้างโปรตีน Glutathione S-Transferase ที่สามารถควบคุมการทำงานของเอนไซม์

โดย ดร. จีรัง ว่องตระกูล และคณะ

สิงหาคม 2548

สัญญาเลขที่ TRG4680035

รายงานวิจัยฉบับสมบูรณ์

โครงการ กรดอะมิโนสำคัญในโครงสร้างโปรตีน Glutathione S-transferase ที่สามารถควบคุมการทำงานของเอนไซม์

คณะผู้วิจัย	สังกัด
1. ดร. จีรัง ว่องตระกูล	มหาวิทยาลัยเชียงใหม่
2. ดร. ละเอียด ประพันธดารา	มหาวิทยาลัยเชียงใหม่
3. Assoc. Prof. Albert J. Ketterman	มหาวิทยาลัยมหิดล

สนับสนุนโดยสำนักงานกองทุนสนับสนุนการวิจัย

(ความเห็นในรายงานนี้เป็นของผู้วิจัย สกว. ไม่จำเป็นต้องเห็นด้วยเสมอไป)

กิตติกรรมประกาศ

งานวิจัยนี้ได้รับการสนับสนุนจากทุนส่งเสริมนักวิจัยรุ่นใหม่ ประจำปี 2546 ของสำนัก งานกองทุนสนับสนุนการวิจัย (สกว) จึงขอขอบพระคุณมา ณ.โอกาสนี้ และ ขอขอบพระคุณผู้อำนวยการสถาบันวิจัยวิทยาศาสตร์สุขภาพ และเจ้าหน้าที่ผู้เกี่ยวข้องทุกท่านที่ได้ให้การสนับสนุนการดำเนินงานโครงการจนสำเร็จลุล่วง

ขอขอบพระคุณนักวิจัยพี่เลี้ยง Assoc. Professor Albert J. Ketterman และ ดร. ละเอียด ประพันธดารา ที่ได้ให้คำแนะนำและเอื้อเฟื้อสารเคมีรวมทั้งคอลัมน์ในการเตรียมเอนไซม์

จีรัง ว่องตระกูล

Abstract

Project Code: TRG4680035

Project Title: Important structural residues of Glutathione S-Transferase control the enzyme function

Investigators: Dr. Jeerang Wongtrakul[*], Dr. La-aied Prapanthadara[*] and Assoc. Prof. Albert J. Ketterman[+]

[*]Research Institute for Health Sciences, Chiang Mai University

[+]Institute of Molecular Biology & Genetics, Mahidol university

E-mail Address: jwongtrakul@yahoo.com, inhso001@chiangmai.ac.th, frakt@mahidol.ac.th

Project Period: 2 years

Glutathione S-transferases (GSTs; EC 2.5.1.18) are a family of detoxifying enzymes that catalyze the conjugation of the sulfhydryl group of glutathione to a wide variety of electrophilic compounds. The GSTs in insect are of particular interest because of their role in insecticide resistance. A knowledge of the structure and function of GSTs is required in order to understand the enzymatic properties. In this study, five mutants of *Anopheles dirus* at position 96, an interface residue, of AdGSTD3-3 and five neighboring residue mutants of the amino acid position 96 were obtained using PCR site directed mutagenesis. The recombinant enzymes were purified using affinity chromatography on a GSTrap column. Differences in the kinetic parameters of the mutants toward the standard substrates CDNB,GSH, inhibitor and insecticides were

observed. Therefore residue changes at an interface position could affect the binding and interaction with those tested compounds. Marked difference in the thermal stability of Arg 96 mutants could be observed. The polar and non-polar residues in this position generate a more stable enzyme than that of the wild type clone, indicating an important role for this residue in structural stabilization. Based on the available crystal structure of the baseline AdGSTD3-3, and the kinetic data, Arg 96 interface residue may affect the interaction with Trp 63 in the other subunit. The positional changes in Trp 63 would then influence the interaction with Gln 49 which is an active site residue in the other subunit and modulate the catalytic activity of AdGSTD3-3.

Keywords: Glutathione transferase, kinetic parameters, site-directed mutagenesis, stability

บทคัดย่อ

รหัสโครงการ TRG4680035

ชื่อโครงการ กรดอะมิโนสำคัญในโครงสร้างโปรตีน Glutathione S-Transferase ที่สามารถควบคุมการทำงานของเอนไซม์

ชื่อนักวิจัย ดร จีรัง ว่องตระกูล[a], ดร. ละเอียด ประพันธดารา[a] และ Assoc. Prof. Albert J. Ketterman[b]

[a]สถาบันวิจัยวิทยาศาสตร์สุขภาพ มหาวิทยาลัยเชียงใหม่

[b]สถาบันอณูชีววิทยาและพันธุศาสตร์ มหาวิทยาลัยมหิดล ศาลายา

E-mail Address: jwongtrakul@yahoo.com, inhso001@chiangmai.ac.th, frakt@mahidol.ac.th

ระยะเวลาโครงการ 2 ปี

กลูตาไธโอนเอสทรานสเฟอเรสเป็นกลุ่มของเอนไซม์ที่มีความสามารถในการทำลายสารพิษโดยการเร่งปฏิกิริยารวมกันของหมู่ sulthydryl ของกลูตาไธโอนกับสารประกอบหลายชนิด GSTในแมลงเป็นที่สนใจเนื่องจากมีบทบาทในการต้านยาฆ่าแมลงการศึกษาเกี่ยวกับโครงสร้างและหน้าที่ของGSTทำให้เข้าใจในคุณสมบัติของเอนไซม์นี้มากขึ้น การศึกษานี้ได้ทำการเปลี่ยนกรดอะมิโนเฉพาะที่ของเอนไซม์ AdGSTD3-3ที่ตำแหน่ง 96 (บริเวณรอยต่อระหว่างโปรตีนสองยูนิท) โดยเปลี่ยนเป็นกรดอะมิโนต่างๆกัน 5 ชนิดและสร้างเอนไซม์กลายพันธ์ของกรดอะมิโนบริเวณใกล้เคียงกรดอะมิโน 96 อีก 5 ตัว เอนไซม์กลายพันธ์ทั้งหมดได้ถูกทำให้บริสุทธ์โดยจับกับ GSTrap column จากการศึกษาทางจลน์ศาสตร์ได้พบความแตกต่างในการทำปฏิกิริยากับสับสเตรท GSH และ CDNB สารยับยั้งต่างๆรวมถึงยาฆ่าแมลง ดังนั้นการเปลี่ยนกรดอะมิโนบริเวณดังกล่าวมีผลต่อการจับกับสารที่นำมาทดสอบ ได้ทำการศึกษาเสถียรภาพต่อความร้อน และพบว่ากรดอะมิโนกลุ่มที่โพ

ลาร์และไม่โพลาร์มีเสถียรภาพต่อความร้อนสูงกว่าเอนไซม์ต้นแบบอย่างมาก ซึ่งชี้ให้เห็นถึงความสำคัญของกรดอะมิโนที่ตำแหน่งนี้ในการคงสภาพโครงรูปของโปรตีน จากการศึกษาโครงสร้างผลึกสามมิติของโปรตีนที่มีอยู่และผลจากการศึกษาทางจลน์ศาสตร์ กรดอะมิโน96อาจจะมีผลต่อกรดอะมิโนใกล้เคียงเช่น Trp 63 ในอีกสับยูนิทและการเปลี่ยนแปลงของ Trp 63 อาจจะกระทบต่อ Gln 49 ซึ่งเป็นกรดอะมิโนบริเวณเร่งของเอนไซม์และ ควบคุมแอคทิวิทีของเอนไซม์

คำหลัก: กลูตาไธโอนเอสทรานสเฟอเรส คุณสมบัติทางจลน์ศาสตร์ การเปลี่ยนกรดอะมิโนเฉพาะที่ เสถียรภาพต่อความร้อน

Executive summary

Project title: Important structural residues of Glutathione S-Transferase control the enzyme function

Principal Investigator: Dr. Jeerang Wongtrakul, Chiang Mai University

Mentors: Assoc. Prof. Albert J. Ketterman and Dr. La-aied Prapanthadara, Mahidol university and Chiang Mai University respectively

Significance and rationale:

Currently 300 million people worldwide are infected by malaria. The mortality rate is between 1 and 1.5 million people per year (WHO, 2002). Thailand is also one of the endemic regions. In the year 2000, there were approximately 90,000 cases of infected people found throughout the country (Malaria division, Department of Communicable Disease Control). Malaria parasites are transmitted to people by the female anopheline mosquito. At present the situation of malaria has become more complex with the increase in resistance to insecticides. Insect Glutathione S-transferases (GSTs) were shown to be involved in the resistance mechanism toward insecticides. It was found that a DDT resistant strain of *An. gambiae*, the major malaria vector in Africa, had increased DDT dehydrochlorinase activity catalyzed by GST. In Thailand, *An. dirus* is a major malaria vector. It has been shown to possess significant amounts of DDT dehydrochlorinase activity. Currently pyrethroid insecticides are being used for the control of insect disease vectors. Resistance towards these insecticides could occur in several ways; such as target site resistance based or metabolism based. In target site

resistance, a single point mutation of the sodium channel was found to confer channel insensitivity to permethrin. In metabolism based, resistance increased gene expression has been observed for the molecular basis of GST resistance in mosquitoes. Indiscriminate use of insecticides will cause more resistance problems in the future. Therefore understanding structure-function relationships of amino acids in insect GSTs is necessary to identify the important residues that affect the enzyme. The results can be used as a basis for better drug design in the future such as for insecticide synergists.

Objectives:

This work aimed to continue the study performed during a Ph.D. research project supported by Royal Golden Jubilee scholarship. In the continuing project, we initially plan to study structure-function relationships of the *An. dirus* GST 1-3 isoenzyme by characterizing an important residue, Arginine 96 (Arg 96) which showed some interesting results in Ph.D. research project. The Arg96Ala mutant possessed changes in activity toward glutathione and CDNB substrates as well as increases in the enzyme stability. Residue Arg 96 was characterized further by replacement with a series of amino acids. In addition, several neighboring residues of Arg 96 such as Tryptophan 63 (Trp 63), Phenylalanine 140 (Phe 140), Asparagine 47 (Asn 47), Proline 48 (Pro 48) and Glutamine 49 (Gln 49) were mutated to elucidate their interactions with Arg 96.

The work was divided into 3 parts.

1. To generate a series of Arg 96 mutants using site directed mutagenesis.
2. To express and characterize all the Arg 96 mutant enzymes using several kinetic parameters e.g. V_{max}, K_m, substrate specificity, percent inhibition and stability

assay. The interpretation of these results was aided by the available crystal structure of adGST1-3.

3. To understand the interaction of Arg 96 with neighboring residues such as Trp 63, Phe 140, Asn 47, Pro 48 and Gln 49 based on the results obtained from part 1 and part 2.

Methodologies

To achieve aim 1:

The adGST1-3 DNA was prepared from our previous construct using Cetylmethylammonium bromide (CTAB) plasmid mini preparation. Mutagenic primers were designed using Vector NTI version 6 software. Then a QuikChange ™ site directed mutagenesis kit (Stratagene) was used to make point mutations. This method was performed using *Pfu* DNA polymerase, which replicates both plasmid strands with high fidelity and without displacing the mutant oligonucleotide primers. The amplification was performed using a Thermal Cycler 2400. The PCR product was treated with *Dpn*I. This enzyme is specific for methylated and hemimethylated DNA and is used to digest the DNA template. The nicked vector DNA incorporating the desired mutations was transformed into *E.coli* by a heat-shock method. The plasmid was screened using restriction enzyme digest. To verify the mutations, DNA sequencing reactions were performed.

To achieve aim 2:

Wild type and mutant enzymes were expressed using pET system. The culture of *E.coli* BL21(DE3)plysS containing a mutant plasmid was grown at 37^{o}C until the OD

600 is approximately 1.0. After induction with IPTG, the cell pellet was collected by centrifugation. The cell pellets were resuspended and lysed by a sonicator. The target protein was purified using GSTrap ^{TM} column. All the steps to obtain the purified GSTs were performed at 4^{o}C. The non-specific binding proteins were removed by washing and the proteins bound to the column were eluted. The fractions containing recombinant GST were concentrated by using a centriprep-10. Then the bound glutathione were eliminated using NAP5 columns. The concentrated protein were eluted and the concentration step were repeated until the final volume is 0.5 ml. Glycerol was added to a final concentration of 50% and the purified concentrated GSTs were stored at –20^{o}C.

The purity of an enzyme preparation were determined by SDS-PAGE using Bio-Rad low range standards as a molecular weight marker. K_m and V_{max} for 1-chloro-2,4-dinitrobenzene (CDNB) and glutathione (GSH) were determined by non-linear regression analysis using Graphad Prism 2.01 software. Specific activities toward a panel of GST substrates; CDNB, 1-2-dichloro-4nitrobenzene (DCNB), ethacrynic acid, 4-nitrophenethyl bromide, were determined spectrophotometrically using the appropriate pH and λ_{max}. Percent inhibition studies was performed using the standard GST assay conditions (10 mM GSH and 1 mM CDNB) in the presence and absence of the various compounds such as Cumene hydroperoxide, DCNB, Deltamethrin, Permethrin and S-hexyl glutathione. The percent inhibition were calculated from a 100% control activity. In the thermal stability assay, the enzymes were prepared at the same concentration. The stability time course of the enzyme at 50^{o}C were determined by withdrawing suitable aliquots from a heating block at different time points for assay of remaining activity.

Protein concentration were determined using the Bio-Rad protein reagent with BSA as the standard protein.

To achieve aim 3:

Residue Trp 63, Phe 140, Asn 47, Pro 48 and Gln 49 nearby Arg 96 in tertiary space as well as neighboring residues in other regions were replaced with alanine. After the purification and characterization, the tertiary structure also was scrutinized to understand the role of the residues in modulating the enzyme function.

Results:

Five mutants at amino acid 96 were generated as well as five neighboring residue mutants of the amino acid position 96. The results indicated that Arg 96 is an important residue in this region because either eliminating, reversing the charge or changing its neighboring residues results in varied kinetic effects on CDNB substrate and stronger effects on GSH substrate e.g. V_{max}, K_m and $K_{cat/km}$. In addition there is a relationship between the amino acid property in position 96 and thermal stability of the AdGSTD3-3, where more non-polar and uncharged residues in this position generate a thermally more stable enzyme. The results suggested that Arg 96 residue at the interface affects the interaction with Trp 63 in the other subunit. The positional changes in Trp 63 would then influence the interaction with Gln 49 which is an active site residue in the other subunit and modulate the catalytic activity of AdGSTD3-3.

Conclusions:

Mutations of an interface-forming amino acid residue of an insect delta class GST have an impact on the stability and catalytic function of AdGSTD3-3 due to

structural perturbations that induce small changes in active site topology that affect binding and catalysis.

Output from this project:

1. The results obtained from this study has been published as indicated below;

Wontrakul J, Sramala I, Prapanthadara L and Ketterman AJ. Intra-subunit residue interactions from the protein surface to the active site of Glutathione S-transferase AdGSTD3-3 impact on structure and enzyme properties. Insect Biochem Mol Biol. 2005 35: 197-205.

2. Some parts of this work were presented in The Thailand Research Fund annual meeting at Karnchanaburi, 14-16 March 2005 as the poster presentation. **Wontrakul J**, Prapanthadara L and Ketterman AJ. Interface Residue, Arg 96, Of Glutathione S-transferase Modulates Enzyme Function.

Introduction

An. dirus mosquito was responsible for over 700 malarial deaths in Thailand in 1997 (1). We are interested in the role of glutathione S-transferases (EC 2.5.1.18; GSTs) in conferring insecticide resistance in this Thai malaria vector. Glutathione S-transferases (GSTs, EC 2.5.1.18), are a heterogeneous family of enzymes that catalyze the conjugation of glutathione (GSH) to elctrophilic sites on a variety of hydrophobic substrates (2). GSTs also play many biological roles in non-enzymatic functions such as catalysis modulation of signal transduction, modulation of ion channels and counter ageing-associated oxidative and chemical stresses etc (3-5). Soluble GSTs have been grouped into many classes, based on similarities in their primary structures, substrate specificity and immunological properties, named alpha, mu, pi, theta, sigma, kappa, omega, kappa, delta, epsilon, zeta etc (6-8). GSTs are cytosolic dimeric proteins comprising two subunits each around 24-28 kDa in size. They share a similar overall folding topology. The active site of a GST is composed of two subsites, the glutathione binding site (G-site) and the hydrophobic substrate binding site (H-site) where the electrophile is bound. The highly conserved G-site binds the tripeptide glutathione (GSH) and is largely composed of amino acid residues found in the N-terminal of the protein. The H-site is more variable in structure and is largely formed from residues from the C-terminus. Examination of structural features at the subunit interfaces of the various gene classes reveals the existence of two major types of interfaces: one that contains a specific hydrophobic intersubunit motif and another that is flat and more hydrophilic (9-14). In insects, GSTs are grouped into six classes based on their amino acid sequences,

namely, theta, zeta, phi, delta, epsilon and omega (15). We are interested in Delta class, formerly classified as class I, which has been implicated in detoxification particulary in conferring resistance toward various insecticides. Based on previous works on our group, the adGST1AS1 gene was identified from an *An. dirus* genomic library (16). The alternatively spliced products of this gene were predicted to produce four mature transcripts which are AdGSTD1-1, AdGSTD2-2 AdGSTD3-3 and AdGSTD4-4. AdGSTD1-1 and AdGSTD3-3, are 630 base pairs and the translated amino acid sequences are 209 residues whereas the length of isoenzyme AdGSTD2-2 and AdGSTD4-4 are 654 base pairs and 650 base pairs respectively. The translated amino acid sequences of the four isoforms shared more than 61% identity. Their amino acid residues at position 1-45 in the N-terminal, shared 100% identity while their C-terminal share more than 51% identity. C-terminal sequence of AdGSTD1-1 has the greatest identity to AdGSTD3-3, 73% while it has 52% and 56% to AdGSTD2-2 and AdGSTD4-4. Among the alternatively spliced products of adGST1AS1 gene, AdGSTD3-3 was the most reactive enzyme in catalyzing CDNB conjugation with the rate of 67 μmol/min/mg (17) therefore this isoenzyme was chosen in this study in order to study structure and function of the enzyme.

Regarding AdGSTD3-3, several active site residues of this enzyme have been studied which are Ile 52, Glu 64, Ser 65, Arg 66 and Met 101 (18). Residue 64 was found to have a role in folding whereas the remaining residues involve in catalytic mechanism and influence in the packing of the protein. There are several reports concerning residue changes not in the substrate binding site can affect the function of

active site residues, including tertiary structure and the catalytic activity of GSTs (19-23). Therefore several structural residues of this insect GST were characterized. The crystal structure of AdGSTD3-3 (11) was used as a tool to guide the structure-function relationship study. The first structural residue that was characterized in AdGSTD3-3 is Cys 69 (24). Nine mutants were generated at this position by replacing the residue with polar, non-polar and charged residues using PCR-based site-directed mutagenesis. All the mutants enzymes were then purified by affinity chromatography and characterized using several kinetic parameters. Molecular dynamics simulations were also performed to understand all the changes in the enzyme structure. The polar residues changed the V_m of the enzymes. With non-polar residues, the enzymes were unable to fold and were expressed in the insoluble inclusion form. With charged residues, the soluble enzyme yields were only 3% of the wild type protein. All Cys69 mutants have dramatically decreased half-lives. therefore residue 69 may be involved in the initial enzyme folding as well as stability. Molecular dynamics simulation also showed that the location of Cys69 mutants relative to the center of gravity of the protein is different for the wild type indicating a different conformation.These findings are additional evidence of the importance of structural residues that affect the enzymatic properties such as V_m, K_m and enzyme specificity.

Additional structural residue of AdGSTD3-3 is Asp 150, a residue located in a loop before helix 6. Analysis of kinetic parameters indicated that Asp150Ser mutant showed marked differences in K_m toward both GSH and CDNB substrates. The mutant also possessed a decreased half-life relative to the wild type enzyme (25). The Asp 150

mutation appears to affect neighboring residues that support two important structural motifs, the N-capping box and the hydrophobic stable motif. The effects of the Asp 150 residue on the active site can be proposed to occur through two pathways; intra-subunit and inter-subunit of the protein. Recently, the intra-subunit pathway was proofed and found that Asp 150 forms an ionic interaction with His 144. As a result, the interaction appeared to stabilized the loop of residues 142-155 between helix 5 and 6. In addition, two conserved hydrophobic residues within the loop, Val 147 and Ala 148 also have van der Waal contact with neighboring residues in the hydrophobic core that support Arg in helix 4. The movement of Arg 96 may influence Arg 66 in the active site (26). This work mainly focuses on a further characterization of interface residue 96 and its neighboring residues. Arg 96 is located in helix 4. The main chain of this residue supports the structure of active site residues 64-66 in helix 3 whereas the side chain of Arg 96 has van der Waal contact with Phe 140, which is a residue in helix 5 in the same subunit and Trp 63 that is located located in α4 of the other subunit. Arg 96 is also close to residue 47-49, Asn 47, Pro 48 and Gln 49 that are near by the GSH binding site in the other subunit (Figure 1 and 2). Arg 96 was found to participate in the intra subunit pathway of residue interaction from Asp 150, located in the loop before helix 6, to Arg 66, which is an active site residue (26). In addition a mutation of Arg96 to Ala significantly increased the half-life of the enzyme to approximately 3 hours at 45°C and increased K_m toward GSH substrates approximately 9.5-fold. To further study the role of this important interface residue Arg 96, the amino acid was replaced with different group of amino acid to assess the contribution of the residue toward the catalytic function as

well as protein conformational stability. In addition, neighboring residues of Arg 96 will be replaced with Ala e.g. Trp 63, Phe 140, Asn 47, Pro 48 and Gln 49.

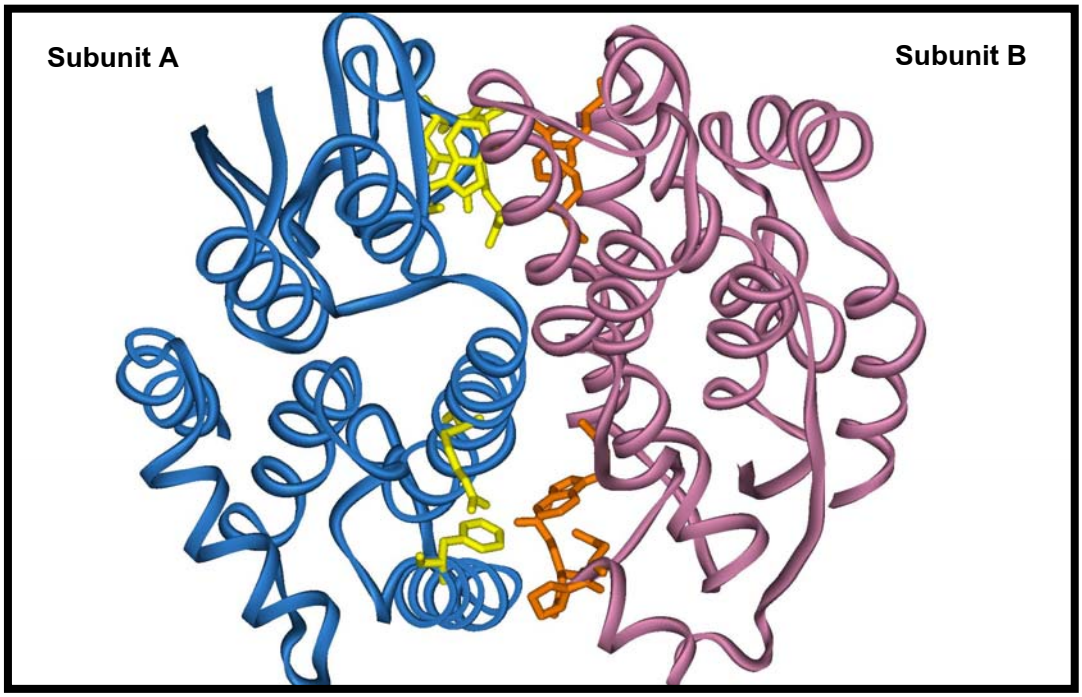

Figure 1: Model of AdGSTD3-3 showing the region of the interface within the dimer.

Amino acid residues of subunit A (blue) are in yellow, and amino acid residues of subunit B (pink) are in orange.

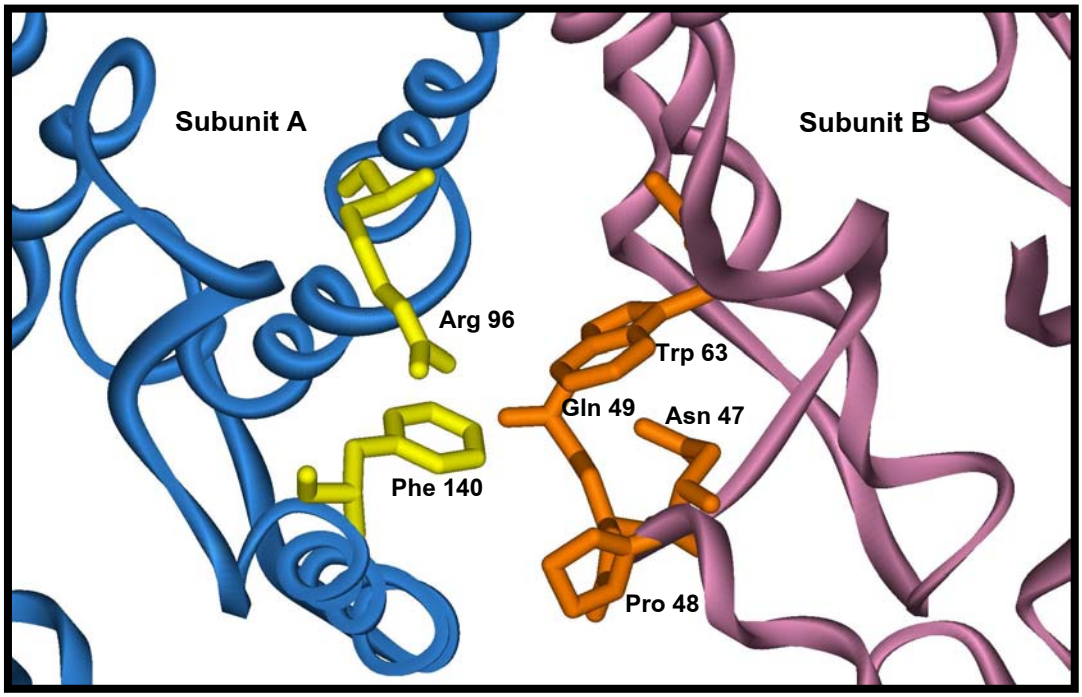

Figure 2: Model of AdGSTD3-3 showing the region of the interface that were studied. Subunit A is in blue, and amino acid side chains of this subunit are in yellow. Subunit B is in pink, and amino acid side chains of this subunit are in orange. The side chain of Arg-96 in one subunit of the protein, shown in a stick representation, interacts with Phe-140 in its own subunit. In addition Arg-96 also interacts with Trp-63 in the other subunit. Both Phe-140 and Trp-63 are located close to Asn-47, Pro-48 and Gln-49 residues which are in the active site in the other subunit.

Methods

1 Preparation AdGSTD3-3 Plasmid DNA Template

Plasmid DNA template of AdGSTD3-3 was prepared from the previous construct (17) which consisted of pET3a containing an insert of AdGSTD3-3 codeding sequence. Plasmid extraction was performed by using Cetyl ammonium bromide (CTAB) method. A single colony of *E.coli* containing the AdGSTD3-3 construct was incubated in 3 ml of LB broth containing 100 µg/ml ampicillin with shaking at 37°C overnight. The culture was transferred to 1.5 ml-microtube and centrifuged at 12,000 rpm for 2 minutes. The supernatant was discarded and the cell pellets were resuspended in 200 µl of STET buffer (8% sucrose, 0.1% TritonX-100, 50 mM EDTA and 50 mM Tris pH 8.0) and mix by vortexing. The resuspended cess were added with 5 µl of 50 mg/ml lysozyme, mixed by vortexing and incubated at room temperature for 10 minutes. The The mixture was boiled at 100°C for 45 seconds and centrifuged at 12,000 rpm for 10 minutes. The cell pellet was removed by using a sterile toothpick. Then 1/10 volume of 5% (w/v) CTAB solution was added, mixed by inversion and let stand for 30 minutes. The mixture was centrifuged at 12,000 rpm for 10 minutes and the supernatant was discarded. The pellet was dissolved with 300 µl of 1.2 M NaCl. In order to remove RNA, 10 µl of RNase (10 mg/ml) was added and incubated at 37°C for 30 minutes. An equal volume of chloroform was added, mixed by inversion and centrifuged at 12000 rpm for 5 minutes. The aqueous phase was transferred to a new 1.5 ml-micro tube and 2 volumes of absolute ethanol were added. After incubation at –80^{o}C for 15 minutes, the mixture was centrifuged at 12,000 rpm for 15 minutes at room temperature. The final DNA pellets

were washed with 70% ethanol. The DNA was briefly air-dried at room temperature, resuspended in 20 μl of sterile distilled water and stored at –20°C.Then the DNA was run on the gel along with the λ *Hind*III marker. The gel was run at 100 volt for 60 minutes then stained with 0.5 mg/ml of ethidium bromide solution in water for 10 minutes and destained with distilled water for 10 minutes. The DNA bands were visualized by ultraviolet irradiation and photographed.

2. Site Directed Mutagenesis of AdGSTD3-3

The method used was based on Stratagene's Quick Change ™ site-directed mutagenesis kit.

2.1. Mutagenesis primer design

The primer sets in these experiments were designed to introduce single mutation at the 96 position of the AdGSTD3-3 sequence to change Arg to five different residues. In addition, five neighboring residue of Arg 96 were chosen and replaced with Ala. All the primers (PROLIGO Primers & Probes) were designed using Vector NTI suite 6 software. Both changed nucleotide and amino acid residues are shown in bold letters. The recognition sites for restriction endonucleases are underlined. Deduced amino acid sequences are shown above the forward primer sequences.

```
                K  R  A  V  V  N  Q  K  L  Y  F  D  M  G
                              HpaI
R96K-F: 5′GAAGCGCGCCGTCGTTAACCAGAAACTGTACTTCGACATGGGC 3′
                                   HpaI
R96K-R: 5′GCCCATGTCGAAGTACAGTTTCTGGTTAACGACGGCGCGCTTC 3′

                K  R  A  V  V  N  Q  E  L  Y  F  D  M
                              HpaI
R96E-F: 5' GAAGCGCGCCGTCGTTAACCAGGAGCTGTACTTCGACAT3'
```

HpaI

R96E-R: 5′ CATGTCGAAGTACAG**CTC**CTGGTTAACGACGGCGCGCTT3′

K R A V V N Q **Y** L Y F D M

HpaI

R96Y-F: 5' GAAGCGCGCCGTCGTTAACCAG**TAC**CTGTACTTCGACAT 3'

HpaI

R96Y-R: 5′ GCCCATGTCGAA**GTA**CAGAAACTGGTTAACGACGGCGCGCTTC 3′

K R A V V N Q **F** L Y F D M G

HpaI

R96F-F: 5' GAAGCGCGCCGTCGTTAACCAG**TTT**CTGTACTTCGACATGGGC 3'

HpaI

R96F-R: 5′ GCCCATGTCGAAGTACAG**AAA**CTGGTTAACGACGGCGCGCTTC 3′

K R A V V N Q **L** L Y F D M

HpaI

R96L-F: 5' GAAGCGCGCCGTCGTTAACCAG**CTG**CTGTACTTCGACATG 3'

HpaI

R96L-R: 5′ CATGTCGAAGTA**CAG**CAGCTGGTTAACGACGGCGCGCTTC 3′

D N G F A L **A** E S R A I

DdeI

W63A-F: 5' GACAATGGCTTTGCGCTG**GCT**GAGTCGCGCGCCATC 3'

DdeI

W63A-R: 5′ GATGGCGCGCGACTC**AGC**CAGCGCAAAGCCATTGTC 3′

K D A V D F L N T **A** L D G H

DraI

F140A-F: 5' GAAGGATGCGGTCGACTTTTTAAACACC**GCT**CTGGACGGGCAC 3

DraI

F140A-R: 5′ GTGCCCGTCCAG**AGC**GGTGTTTAAAAAGTCGACCGCATCCTTC 3′

H M K P E F L K I **A** P Q H C

N47A-F: 5' CACATGAAGCCGGAGTTCCTGAAGATT**GCC**CCCCAACACTGT 3′

N47A-R: 5′ ACAGTGTTGGGG**GGC**AATCTTCAGGAACTCCGGCTTCATGTG 3′

M K P E F L K I N **A** Q H C I

P48A-F: 5' ATGAAGCCGGAGTTCCTGAAGATTAAC**GCC**CAACACTGTATT 3′

P48A-R: 5′ AATACAGTGTTG**GGC**GTTAATCTTCAGGAACTCCGGCTTCAT 3′

K P E F L K I N P **A** H C I P

Q49A-F: 5' GAAGCCGGAGTTCCTGAAGATTAACCCC**GCC**CACTGTATTCCG 3′

Q49A-R: 5′ CGGAATACAGTG**GGC**GGGGTTAATCTTCAGGAACTCCGGCTTC 3′

Remark: Mutation of AdGSTD3-3 at amino acid positions 47, 48 and 49 abolished *EcoRI* restriction site.

Plasmid template DNA, approximately 200 ng was added to the 50 µl reaction mixture that contained 10 pmol of each primer, 2.5 mM each of dNTPs, 1X pfu DNA polymerase buffer (20 mM Tris-HCl, pH 8.8, 10 mM KCl, 10 mM (NH4)2SO4, 100 µg/ml nuclease-free BSA, 0.1% Triton-X 100), 1.5 U of pfu DNA polymerase (Promega). The PCR cycling parameter were, 1 cycle of 30 sec. at 95°C, followed by 16 cycles of 30 sec at 95°C, 1 min at 55°C, and 11 min at 68°C. The PCR products were analyzed by 1% agarose gel electrophoresis.

The parental template DNA was removed by treating the reaction with *Dpn*I, which specifically digested the in vivo methylated parental template. One microliter of DpnI (Promega) was added to the PCR reaction mixture and incubated at 37°C for 1 hour.

2.2 Transformation of PCR Products into *E. coli*

100 ng of DNA after DpnI treated was added to 200 µl of competent cells and incubated on ice for 1 hour. The tubes were transferred to a preheated 42°C circulating water bath. The cells were heat-shocked at 42°C for exactly 90 seconds and rapidly transferred on ice for 5 minutes. The transformed cells were added to 800 µl of LB broth and incubated for 1 hr in a shaking incubator at 37°C for 1 hour to allow the bacteria to recover. 200 µl of transformed competent cells were spread onto agar medium containing an appropriate antibiotic. The plates were incubated at 37^{o}C for 12-16 hours. Aproximately ten clones of each mutant were randomly selected for restriction analysis.

Digestion of plasmid DNA was performed consisting of 2 µl DNA, 1 µl of restriction enzyme corresponding to the restriction recognition site introduced in the mutagenic primer, 2 µl of 10X buffer and 15 µl of sterile distilled water in a 1.5 micro centrifuge tube. The tubes were incubated at an appropriate temperature depending on the enzyme used for 2-3 hours. Then the DNA was run on 1% agarose gel. The desired plasmid DNA clone was stored at -20°C.

2.3 DNA sequencing

The DNA sequencing reactions were performed using T_7 promoter universal primers with ABI PRISM Bigdye™ Terminator or Cycle Sequencing Ready Reaction Kit (Perkin Elmer), following the manufacturer's instructions. Twenty-five cycles of PCR for sequencing were performed using the following conditions; the denaturing step at 96°C for 10 seconds, the annealing step at 50°C for 5 seconds and the extension step at 60 °C for 4 minutes. The products from thermal cycling were transferred to a new 0.5 ml-microtube and added to 80 µl of sterile distilled water, 1/10 volume of 3 M sodium acetate and 2.5 volume of 95% ethanol. The mixture was incubated 30 minutes at room temperature and spun at 12,000 rpm for 15 minutes. The pellet was washed with 70% ethanol and dried for 1 hr. Then the correct mutant DNA was transformed into *E. co*li BL21 (DE3)pLysS and plated on LB agar plate containing 100 µg/ml ampicillin and 34 µg/ml chloramphenicol. The LB agar plates were incubated at 37°C overnight.

3. Expression and purification of recombinant Clones

E.coli BL21De3plys cells harbouring mutant plasmid were grown at 37ºC in Luria-Bertani medium containing 100 mg/ml ampicillin and 34 mg/ml Chloramphenicol. The synthesis of GST was induced by the addition of 1 mM isopropyl thio-β-D-galactoside when the absorbance at 600 nm was 1.0. Three hours after induction, cells were harvested by centrifugation at 7000 rpm for 20 minutes, resuspended in PBS, sonicated and centrifuged at 10,000 rpm for 20 minutes. The supernatant was collected for further step.

The recombinant GST, which expressed as a soluble protein in the supernatant of total cell lysate was purified by using GSTrap affinity chromatography, according to the manufacturer's instructions. The column was equilibrated with 5 column volumes of the binding buffer, PBS pH 7.3. Total cell lysate was passed through sterile filter with 0.45 μm cut-off and then applied to the column. Subsequently, the column was washed with 5 to 7 column volumes of the same binding buffer. To eluate the bound recombinant GST, 4 column volumes of elution buffer (10 mM GSH in 1.5 M Tris-HCl pH 8.0, and 10 mM DTT) was applied to the column. All of the buffer passing through the column at each step was collected for further characterization, and all the steps were performed at 4°C. Every fraction containing recombinant GST was pooled before concentrating. The target protein was concentrated until the final volume less than 1 ml. Concentrating was performed by centrifuging a Centriprep-10 at 2,500 X g at 4°C. Glutathione that bound to the recombinant GST was eliminated by using NAP-5 column. Two NAP-five columns were equilibrated with 5 column volumes of 50 mM phosphate buffer pH 6.5. Then, 0.5 ml of the concentrated protein was applied to the column each

while the effluents were collected. The purified protein was eluted with 1 ml of the same equilibrating buffer containing 10 mM DTT. Then both eluted fractions were pooled and the concentrating step was repeated as previously described, until the final volume of the protein reach 0.5 ml. The purified enzyme was stored at -20°C in 50% glycerol until use. All the step were performed at 4°C.

4. Kinetic studies

GST activities were measured spectrophotometrically in 1-ml quartz cuvettes in a Shimadzu UV-2101PC spectrophotometer. Steady-state kinetic measurements were performed at 25°C in 0.1 M potassium phosphate buffer pH 6.5. Initial velocities were determined in the presence of 10 mM GSH and CDNB was used in the concentration range of 0.02 mM to 3.0 mM. Alternatively, CDNB was used at a fixed concentration (1mM), and the GSH concentration was varied in the range of 0.008 mM to 15.0 mM. Specific activities toward different substrates were performed (27). The activity with 1 mM 1-chloro-2, 4-dinitrobenzene (CDNB) was measured by at 340 nm at pH 6.5, using a molar absorption coefficient of 9.6 $mM^{-1}cm^{-1}$. The activity with 1mM 1,2-dichloro-4-nitrobenzene (DCNB) was measured by 345 nm at pH 7.5, using a molar absorption coefficient of 8.5 $mM^{-1}cm^{-1}$. 4-nitrophenethyl bromide was used at 0.1 mM concentration and the reaction was monitored at 310 nm; using pH 6.5 and a molar absorption coefficient of 1.2 respectively. A final substrate, Ethacrynic acid, was used at 0.2 mM and the reaction was monitored at 270 nm; using pH 6.5 and a molar absorption coefficient of 5.0. GSH stock solutions were prepared in 0.1 M phosphate buffer using

the appropriate pH for each substrate. All the stock hydrophobic substrates were prepared in absolute ethanol and diluted into the assay buffer. All measurements were performed at 25-27^{o}C in 0.1 M phosphate buffer. Specific activities were calculated based on the molar extinction coefficient for each substrate. The specific activities reported are the mean ± standard deviation for at least three independent assays. Using (0.01-0.1 mM) S-hexyl glutathione, (0.001-0.1 mM) Ethacrynic acid, 0.1 mM p-nitrophenethyl bromide, 2.5 mM cumene hydroperoxide, 1 mM 1,2-dichloro-4-nitrobenzene (DCNB), (0.01-0.1 mM) BSP, 0.01 mM permethrin and deltamethrin. The inhibition studies were performed using the standard GST assay conditions (10 mM GSH and 1 mM CDNB) in the presence and absence of the inhibitors. The inhibitors were prepared in absolute ethanol except S-hexyl GSH was resuspended in phosphate buffer pH 6.5. The percent inhibition was calculated based on the activity of the enzyme with no inhibitor as 100%.

5. Stability assay

Thermal stability was measured as a function of time. All the wild type AdGSTD3-3 and mutant enzymes were incubated (0.1 mg/ml in 0.1 M potassium phosphate pH 6.5 containing 5 mM DTT and 1 mM EDTA) at 50 °C and aliquots were assayed for activity in the standard system at different time-points. Half-lives for the enzymes represent the time of incubation when there is 50% residual activity and were calculated using the equations: Slope = k/2.3, $k = 0.693/t_{1/2}$. The slope was obtained

from the linear plot between log percentage of original activity and the time point of preincubation using GraphPad Prism 4 .

Results

1. Arg96 Mutant Expression and Purification

All the Arg96 mutants were generated with correct sequences as planned. It was found that Arg96Ala, Arg96Lys, Arg96Phe, Arg96Tyr and Arg96Leu mutants were expressed in *E.coli* at 37°C with a band size of approximately 23 kDa. The yields of soluble protein range from 16-31% of total soluble protein from the bacterial lysate (Table 3). There was one mutant, Arg96Glu that expressed GST in an insoluble inclusion form. The expression temperature was reduced to 25°C. However, the GST was expressed at a relatively low level approximately 7% of the total protein in the lysate. The purified protein of Arg96Glu gave a single band on SDS gel with a size as expected.

Table 3 Purification of the Arg 96 mutant proteins

Enzymes	Step	Total protein (mg)	Yield (%)	Total activity (μmol/min)	Specific activity (μmol/min/mg)
Wild type	Lysate	44	100	5918	135
	Purified	14	31	554	40
Arg96Ala	Lysate	64	100	1065	17
	Purified	12	19	375	32

Arg96Lys	Lysate	35	100	203	6
	Purified	6	17	165	44
Arg96Phe	Lysate	81	100	1967	24
	Purified	20	25	536	27
Arg96Tyr	Lysate	81	100	1698	21
	Purified	24	30	722	30
Arg96Leu	Lysate	73	100	2486	34
	Purified	27	37	1192	44
Arg96Glu	Lysate	39	100	260	7
	Purified	3	7	143	54

2. Expression and Purification of Arg 96 neighboring residues

All the mutant enzymes were expressed started with 37ºC temperature and purified using GST affinity column. The yields of all soluble proteins were shown in Table 4. The yields of Arg 96 neighboring residues ranged from 2 to 31% of total soluble protein in the bacterial lysate. It was found that Asn47Ala mutant showed no catalytic activity in the lysates. SDS polyacrylamide gel electrophoresis was performed and confirmed that both enzymes expressed as insoluble inclusion bodies. Therefore an induction temperature was lowered to 25ºC as of the Arg96Glu. The mutant enzyme was expressed in soluble form and demonstrated detectable activity in the lysate. In contrast to the Arg96Glu mutant, the Asn47Ala mutant enzymes failed to bind neither GSTrap nor an S-hexylglutathione affinity suggesting that the amino acid at this position

is essential for an initial enzyme folding. Since the information from the remaining mutants are enough to explain the function of residue 96. So the purification of Asn47Ala mutant is terminated.

Table 4 Purification of the Arg 96 neighboring residues

Enzymes	Step	Total protein (mg)	Yield (%)	Total activity (μmol/min)	Specific activity (μmol/min/mg)
Pro48Ala	Lysate	50	100	545	11
	Purified	12	24	158	13
Gln49Ala	Lysate	47	100	878	19
	Purified	15	31	363	25
Trp63Ala	Lysate	14	100	19	1.3
	Purified	0.3	2	5	15
Phe140Ala	Lysate	38	100	367	10
	Purified	3	8	57	19

3. Stability assay

The amino acid property of the side-chain at position 96 is of importance for thermal stability at 50ºC as shown in Figure 3. Removal of the guanidine group of Arg 96, which gives mutant Arg96Ala, leads to a more stable enzyme with a 9.8-fold increase in half-life. The replacement of the guanidine group with lesser positively charged residue lysine did not affect on the enzyme half-life. Replacing the Arg in

position 96 by negatively charged Glu residue slightly increased the half-life of the enzyme. Therefore charged residues at position 96 had no stabilizing effect on the AdGSTD3-3 isoenzyme. On the other hand, replacement of Arg 96 with either phenolic or phenolic hydroxyl group of Phe and Tyr, which give mutant Arg96Phe and Arg96Tyr, leads to a significant more stable enzyme with a 14-fold increase in half-life compared with the wild type. In addition, the change of Arg 96 with an aliphatic side chain Leu significantly increased the half-life 27-fold compared to the wild type AdGSTD3-3. Among the remaining four neighboring residues of Arg 96 that were targeted in this study, Phe140 and Trp 63 residues significantly affected the stability of the enzymes. The site-directed replacement of both residues with alanine reduced the half-life to 47 and 35% compared to the wild type respectively. The results also correlated with the protein yields obtained after the enzyme purification. The yields of Trp 63 and Phe 140 were 25-50% of the wild type protein Table 2, suggesting that both enzymes are temperature sensitive mutants. A relationship between the amino acid property in position 96 and thermal stability of the AdGSTD3-3 seems to exist, where more non-polar and uncharged residues in this position generate a thermally more stable enzyme. A longer incubation of Arg96Phe and Arg96Tyr mutants at 45°C showed that both proteins retained their activities more than 10 hours (data not shown).

4. Kinetic parameters

All the kinetic parameters were studied by varying concentrations of both GSH and CDNB substrates. The reactions followed Michaelis-Menten. Kinetic parameters were

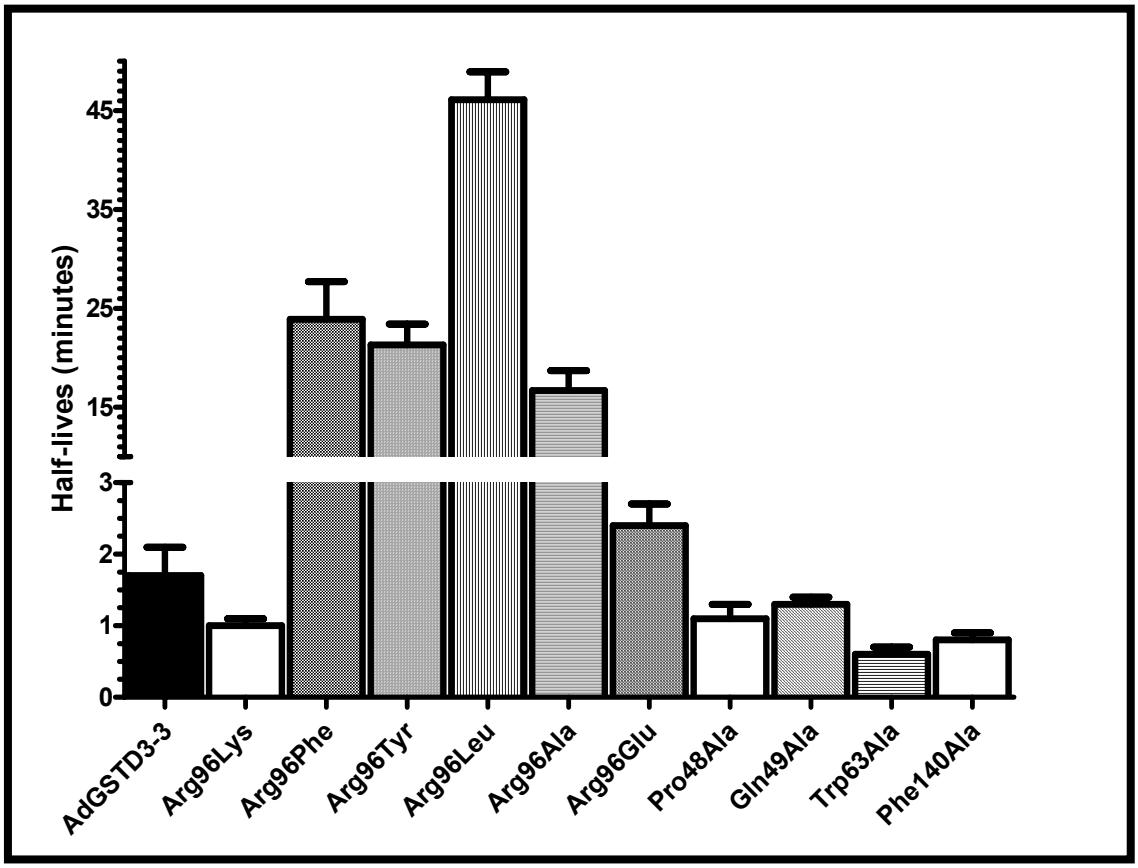

Figure 3: Half-lives of Arg 96 and its mutants at 50ºC. Half-life represents the time of incubation after which 50% activity remains measured in the standard assay system, the conjugation between CDNB (1 mM) and GSH (10 mM)

determined by non-linear regression analysis using GraphPad Prism software version 4. Comparison of the kinetic parameters of Arg 96 mutants and neighboring residue mutants values showed that the residue change affected enzymatic properties (Table 5 and 6). When Arg 96 is replaced with Leu, Ala and Glu residues, the K_m for CDNB increases markedly 1.8 to 3.8-fold (Table 5). In addition, the K_m toward GSH change notably 2.2 to 20.5-fold for all of the mutants of Arg 96 residue suggesting a decreased binding affinity of the mutants toward GSH substrate (Table 6). The replacement of Arg 96 with Glu and Phe caused the increase in Vmax toward CDNB and GSH substrates 1.9-fold and 3.1-fold, respectively, compared to the wild type. The catalytic efficiency (K_{cat}/k_m) of Arg96Phe toward CDNB was 1.3-fold greater than the wild type enzyme, whereas the K_{cat}/K_m of Arg96Ala was 4.6-fold lesser than the wild type. For GSH substrate, the catalytic efficiency of Arg96Lys, Arg96Tyr, Arg96Leu and Arg96Ala mutants were 1.8 to 12.8-fold less than the wild type enzyme whereas the remaining Arg 96 mutants possessed similar values as the wild type.

The results of steady-state kinetic measurements for enzymes with replacements at the neighboring residues of Arg 96 are given in Table 5 and 6. There is no major changes in the K_m values for CDNB for Pro48Ala mutant. However there is a small increase $K_{m\ CDNB}$ values for Gln49Ala and Phe140Ala mutants. For the $K_{m\ GSH}$, all the Arg96 neighboring residue mutants increased the values ranged from 1.6-fold to 4.5-fold. The catalytic efficiencies toward CDNB and GSH of the neighboring residues mutant were all decreased when compared to the wild type. These results indicated that Arg 96 is an important residue in this region because either eliminating, reversing the

charge or changing its neighboring residues results in varied kinetic effects on CDNB substrate and stronger effects on GSH substrate e.g. V_{max}, K_m and K_{cat} / k_m.

Table 5: Kinetic constants for Arg 96 mutants and its neighboring residue mutants toward CDNB substrate.

Enzymes	V_{max} CDNB at 10 mM GSH	k_{cat}	CDNB	
			K_m	k_{cat}/K_m
AdGSTD3-3	29.3 ± 0.2	11.6	0.13 ± 0.02	89.2
Arg96Lys	26.3 ± 1.8	10.4	0.12 ± 0.02	86.7
Arg96Phe	47.2 ± 1.8	18.7	0.16 ± 0.01	116
Arg96Tyr	39.7 ± 3.3	15.7	0.16 ± 0.02	98.1
Arg96Leu	52.7 ± 2.6	20.8	0.25± 0.04	83.2
Arg96Ala	24.7 ± 1.1	9.75	0.50 ± 0.04	19.5
Arg96Glu	54.9 ± 4.1	21.7	0.24 ± 0.03	90.4
Pro48Ala	22.7 ± 1.0	8.99	0.15 ± 0.04	59.9
Gln49Ala	53.8 ± 1.1	21.3	0.42 ± 0.04	50.7
Trp63Ala	9.20 ± 0.1	3.63	0.07 ± 0.02	50.4
Phe140Ala	27.9 ± 2.7	11.0	0.30 ± 0.02	36.7

The units are: V_{max}: μmole/min/mg, K_m: mM, k_{cat}: s^{-1}, k_{cat}/K_m: $mM^{-1}s^{-1}$. The data are mean ± standard deviation from at least 3 independent experiments.

Table 6: Kinetic constants for Arg 96 mutants and its neighboring residue mutants toward GSH substrate.

Enzyme	V_{max} GSH at 1 mM CDNB	k_{cat}	GSH	
			K_m	k_{cat}/K_m
AdGSTD3-3	19.0 ± 1.8	7.5	0.20 ± 0.06	37.5
Arg96Lys	23.3 ± 1.5	9.2	0.44 ± 0.05	20.9
Arg96Phe	59.4 ± 1.2	23.5	0.61 ± 0.04	38.5
Arg96Tyr	42.0 ± 2.9	16.6	0.63 ± 0.04	26.3
Arg96Leu	38.6 ± 4.3	15.3	0.60 ± 0.06	25.5
Arg96Ala	30.3 ± 3.0	12.0	4.1 ± 0.50	2.93
Arg96Glu	46.1 ± 2.8	18.2	0.49 ± 0.02	37.1
Pro48Ala	23.6 ± 1.8	9.3	0.33 ± 0.04	28.2
Gln49Ala	43.0 ± 3.6	17.0	0.90 ± 0.10	18.9
Trp63Ala	5.56 ± 1.5	2.2	0.33 ± 0.04	6.67
Phe140Ala	28.4 ± 3.5	11.2	2.0 ± 0.2	5.60

The units are: V_{max}: μmole/min/mg, K_m: mM, k_{cat}: s^{-1}, k_{cat}/K_m: $mM^{-1}s^{-1}$. The data are mean ± standard deviation from at least 3 independent experiments.

5. Substrate specificity

Specific activities toward several GST substrates were determined and shown in Table 7. The activity was measured with glutathione and four different substrates (Figure 4) at the appropriate pH and λ_{max}. The compounds were chosen in order to monitor the effect of the structural change on the ability to utilize substrate from different GST classes. CDNB, a general substrate for GSTs, is the substrate that yielded the highest conjugating activity with Phe140Ala mutant having the greatest activity and Trp63Ala the lowest activity. The compound 4-nitrophenethyl bromide and ethacrynic acid are human theta and pi class substrates respectively. All mutants had no activity toward 4-NBC as well as the wild type. Only Arg96Phe, Arg96Tyr and the four neighboring residue mutants had detectable activities to ethacrynic acid. The conjugating activity of Arg96Glu and Phe140Ala towards DCNB, the mu class substrate, was approximately 2.3-fold more than the wild type. The data demonstrated that the change of single residue at the interface resulted in a change of enzyme specificity.

6. **Inhibition study**

The inhibition study was performed using eight different compounds as the inhibitors. Several of the compounds are GST substrates or pyrethroid insecticides. The assays were carried out by using a standard GST assay in the presence and absence of the inhibitors. Of the four compounds tested as substrates from Table 7, only CDNB, DCNB and EA substrates can be utilized by the enzymes. However 4-NPB-Br interacted with Arg 96 mutant enzymes and its neighboring residue mutants as observed by their inhibition of CDNB activity. The same concentration of the compound as was used for

Enzyme	CDNB (1 mM)	DCNB (1 mM)	4-nitrophenethyl bromide (0.1 mM)	Ethacrynic Acid (0.2mM)
AdGSTD3-3	24.7 ± 2.3	0.0333 ± 0.0149	ND	ND
Arg96Lys	43.5 ± 6.4	0.0321 ± 0.002	ND	ND
Arg96Phe	42.3 ± 8.2	0.0622 ± 0.003	ND	0.0042 ± 0.0019
Arg96Tyr	26.9 ± 4.5	0.0362 ± 0.015	ND	0.0028 ± 0.0007
Arg96Leu	34.0 ± 6.2	0.0264 ± 0.007	ND	<0.006
Arg96Ala	28.3 ± 3.7	0.0233 ± 0.003	ND	<0.001
Arg96Glu	40.3 ± 1.6	0.0711 ± 0.016	ND	<0.15
Pro48Ala	32.7 ± 1.2	0.0412 ± 0.002	ND	0.0093 ± 0.0049
Gln49Ala	47.6 ± 5.6	0.0253 ± 0.011	ND	0.0085 ± 0.0018
Trp63Ala	13.8 ± 0.4	0.0201 ± 0.008	ND	0.0361 ± 0.0061
Phe140Ala	58.1 ± 0.35	0.0774 ± 0.006	ND	<0.012

Table 7: Specific activity of Arg 96 and its mutants towards four different substrates.

The units are μmole/min/mg of protein. The data are mean ± standard deviation from at least 3 independent experiments. ND: not detectable

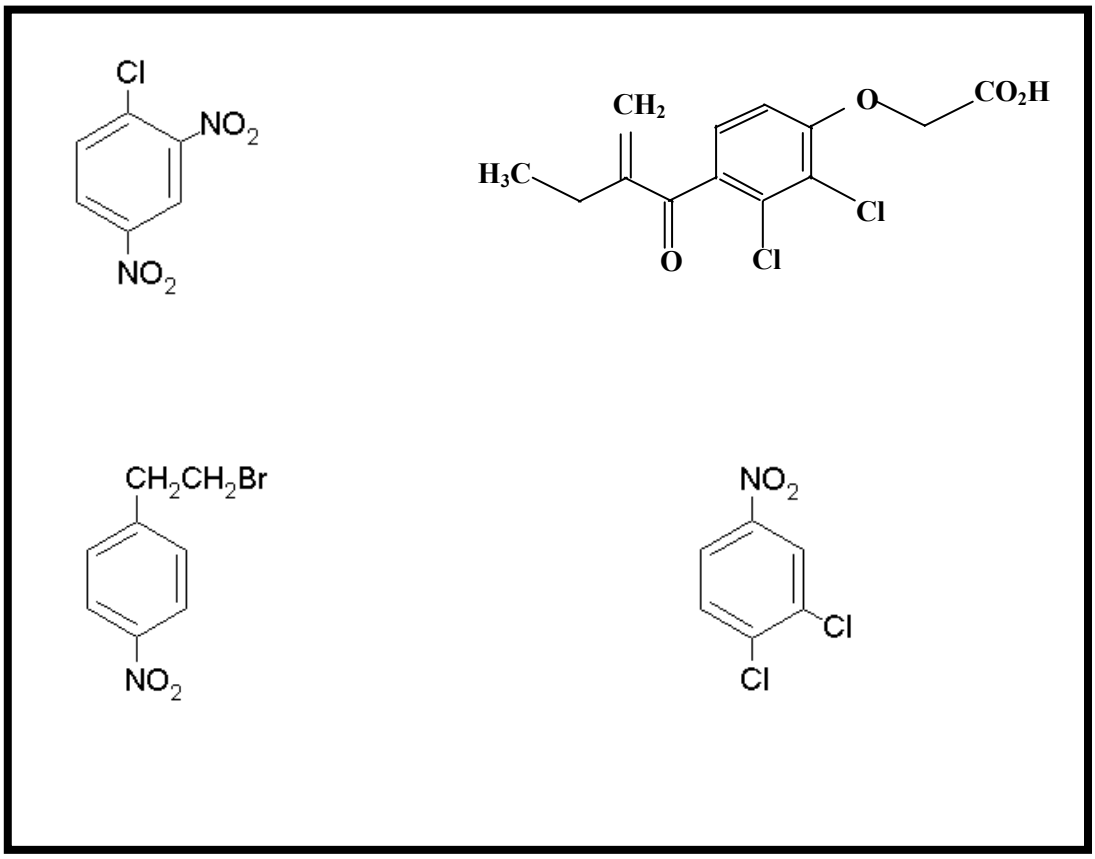

Figure 4 Compounds that are substrates of GSTs.

(A) CDNB: 1-chloro-2,4-dinitrobenzene; (B) ethacrynic acid (C) 4-NPB: 4-nitrophenethyl bromide ; (D) DCNB: 1,2-dichloro-4-nitrobenezene

Table 8: Percent inhibition study of Arg 96 and its mutants from at least three separate experiments.

	0.1 mM BSP	0.01 mM BSP	2.5 mM CuOOH	0.1 mM DCNB	0.1 mM 4-NPB-Br	0.01 mM Delta	0.01 mM Permet	0.1 mM EA	0.01 mM EA	0.001 mM EA	0.1 mM S-hexyl	0.01 mM S-hexyl
WT	92.6 ± 8.2	71.9 ± 15	58.3 ± 2.8	15.1 ± 7.4	39.0 ± 7.1	79.1 ± 6.9	81.0 ± 2.3	92.0 ± 5.7	79.1 ± 9.2	41.0 ± 8.0	76.5 ± 4.9	15.6 ± 2.6
Arg96Lys	98.6 ± 1.3	80.6 ± 2.3	69.5 ± 6.2	38.4 ± 8.2	57.5 ± 3.1	86.6 ± 8.5	75.8 ± 8.0	98.8 ± 1.8	76.8 ± 7.4	55.5 ± 6.1	77.0 ± 3.7	46.1 ± 2.9
Arg96Phe	96.8 ± 1.4	58.9 ± 4.8	45.6 ± 2.9	16.0 ± 4.0	21.7 ± 7.8	37.3 ± 3.3	43.9 ± 9.1	97.0 ± 1.6	63.2 ± 12	15.3 ± 3.8	68.4 ± 5.6	22.7 ± 3.5
Arg96Tyr	96.1 ± 0.6	59.4 ± 8.7	48.4 ± 8.2	9.6 ± 2.7	27.1 ± 13	62.0 ± 3.5	50.8 ± 4.0	94.4 ± 2.6	58.7 ± 5.2	25.4 ± 6.1	75.0 ± 2.6	25.1 ± 9.9
Arg96Leu	98.7 ± 0.8	68.7 ± 9.8	49.5 ± 7.2	23.2 ± 11	28.8 ± 16	54.5 ± 9.0	27.4 ± 8.0	96.6 ± 2.9	53.9 ± 5.1	17.5 ± 6.3	70.8 ± 10	17.1 ± 4.8
Arg96Ala	95.7 ± 5.2	76.0 ± 3.2	66.6 ± 7.6	36.4 ± 15	48.9 ± 12	89.0 ± 5.3	80.2 ± 5.0	97.8 ± 1.2	76.2 ± 4.9	24.4 ± 2.8	80.1 ± 2.7	34.7 ± 9.5
Arg96Glu	99.4 ± 0.8	69.3 ± 7.4	69.4 ± 3.0	31.3 ± 6.5	34.5 ± 5.6	66.9 ± 3.8	68.4 ± 6.8	99.7 ± 0.4	72.2 ± 2.4	30.3 ± 3.0	78.5 ± 2.1	23.3 ± 5.8
Pro48Ala	97.7 ± 2.1	73.5 ± 2.6	59.6 ± 11	39.0 ± 1.4	46.8 ± 9.3	62.5 ± 7.4	34.8 ± 8.8	97.9 ± 0.6	78.0 ± 2.6	37.7 ± 4.9	49.1 ± 6.4	13.8 ± 10
Gln49Ala	99.8 ± 1.9	69.7 ± 6.7	16.7 ± 11	9.8 ± 9.2	16.6 ± 10	44.5 ± 6.8	54.7 ± 15	95.4 ± 1.1	75.7 ± 3.9	26.9 ± 13	59.7 ± 8.7	10.6 ± 7.8
Trp63Ala	96.8 ± 4.4	81.9 ± 5.2	54.2 ± 10	52.8 ± 10	42.5 ± 1.6	57.8 ± 7.5	45.5 ± 5.7	96.4 ± 3.2	75.3 ± 3.2	36.1 ± 8.4	86.1 ± 4.1	7.8 ± 6.3
Phe140Ala	99.8 ± 0.1	89.8 ± 3.2	68.4 ± 7.2	59.3 ± 12	56.8 ± 10	61.3 ± 1.5	61.2 ± 8.6	97.7 ± 2.3	76.4 ± 5.0	50.4 ± 7.4	84.5 ± 5.9	41.7 ± 7.4

The final concentrations of tested compounds are: 0.01-0.1 mM BSP, Bromosulfophthalein, 2.5 mM CuOOH, Cumene hydroperoxide, 1 mM DCNB, 1,2—dichloro-4-nitrobenzene, 0.1 mM 4-NPB-Br, 4-nitrophenethyl bromide, 0.01 mM deltamethrin, permethrin, 0.001-0.1 mM EA, Ethacrynic acid, 0.01-0.1 mM S-hexyl glutathione.

their substrate specificity to study the inhibitory effects (Table 8). In addition, five more compounds were examined interaction with the enzymes. Both 4-NPB-Br and EA interacted with Arg 96 mutants and inhibited them to different levels. Arg96Lys mutant interacted with several compound tested e.g. BSP, DCNB, 4-NPB-Br, EA and S-hexyl-glutathione by showing the relatively high percentage of inhibition, suggesting that the Arg96Lys bound to the compounds and be inhibited more than other Arg 96 mutants. This may be the role of positively charge residue at this position. In contrast, replacing Arg 96 with a phenolic and an aliphatic side chain reduced the binding between the Arg 96 mutants and some compounds. Arg96Phe possessed the lower percent inhibition toward BSP, CuOOH, 4-NPB-Br, deltamethrin and EA whereas Arg96Leu had lower percent inhibition toward permethrin compared to the wild type. For the inhibition study of neighboring residue mutants, Phe140Ala has increased the interaction with the majority of compounds tested e.g. BSP, CuOOH, DCNB, 4-NPB-Br, EA and S-hexylglutathione by demonstrating the highest percent inhibition while replacing Gln 49 with Ala decreased the enzyme-compound interaction.

Discussion

Many interface residues in proteins have been studied and found that they have the roles in several functions e.g. protein folding, contribution to binding affinities, communication through a network of interactions etc (28). In GSTs, there are two major types of protein interface, lock and key type and flat type. The first type is found in alpha, mu and pi classes (21;29;30). The residues at both lock and key positions have been extensively studied including the folding mechanism. In contrast, the latter type is found only in sigma and delta classes (10;11). Only few studies have been done in site directed mutagenesis of interface residues. The majority of studies focused on the folding and refolding mechanism compared to the lock and key interface classes. Based on amino acid alignment of GSTs in alpha, mu and pi compared with delta AdGSTD3-3 class GSTs (Figure 5), the interface residue Arg96 of AdGSTD3-3 is corresponding to Met 92 residue in alpha and pi class or Ile 92 in mu class GST which are the lock residues in those GST mammalian classes. In addition, Gln 49 of AdGSTD3-3 is equal to the Tyr 50 or Phe 50 of the alpha, mu and pi key residue (30). Therefore this subunit structure suggested that the both the mammalian and insect GSTs have shared the common ancestor. This study suggested that the mutation of an interface amino acid of delta class have an effect on the stability and catalytic activity of AdGSTD3-3.

Arg 96 residue not only has a series of residue interaction in the intra subunit of the protein (26), it also affects the interaction with Trp 63 in the other subunit as proposed in Figure 6. The positional changes in Trp 63 would then influence the interaction with Gln 49 which is an active site residue in the other subunit. The similar mechanism is found in maize theta class GST. Asn 49, an interface residue, functioned

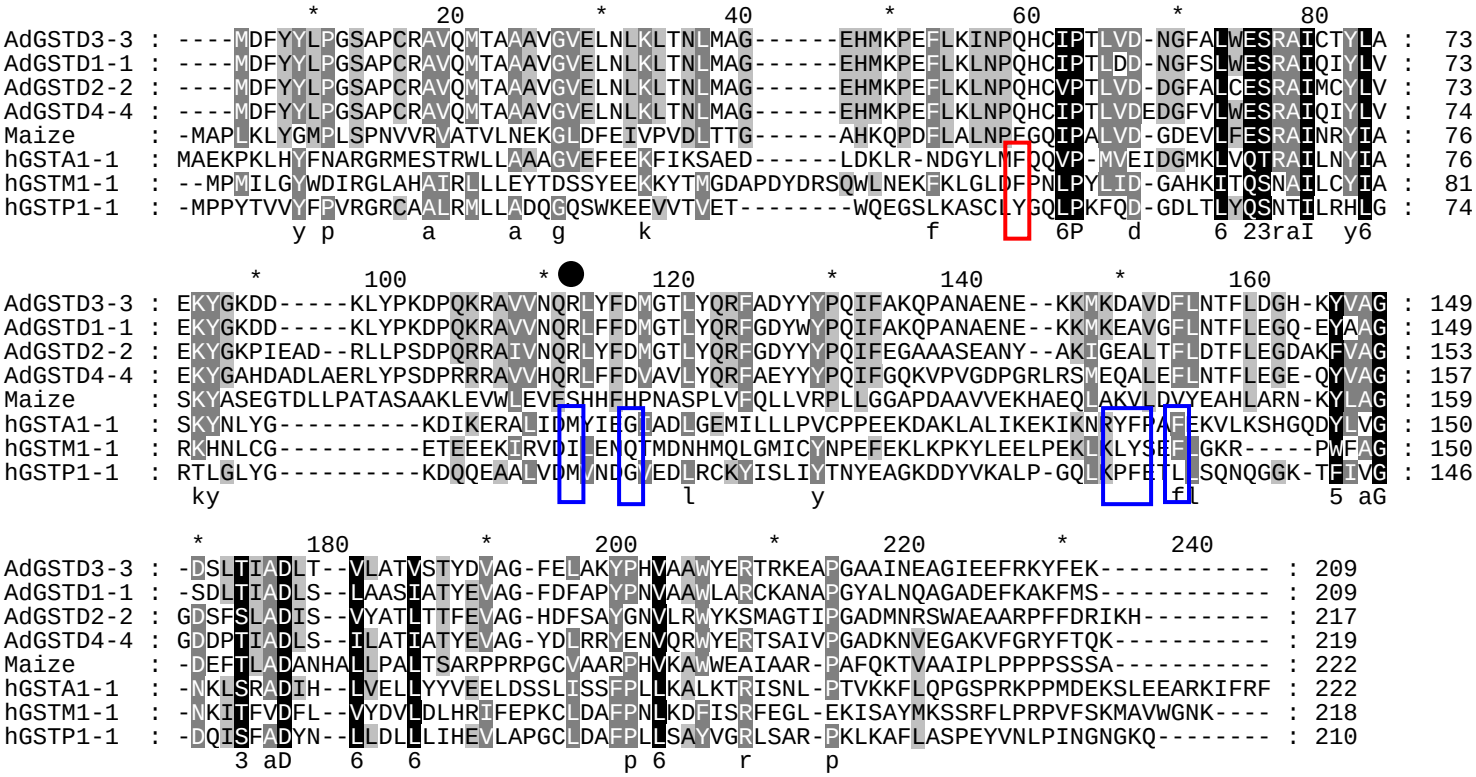

Figure 5: Alignment of topologically equivalent amino acid residues of GSTs from different classes.

Residue numbering for each sequence is shown at the right. Black and dark gray shadings represent 100% and 80% sequence similarity respectively. The sequences have the following Genbank accession numbers: AdGSTD3-3(AAG38505.1), AdGSTD1-1 (AAG38507.1), AdGSTD2-2 (AAG38504.1), AdGSTD4-4 (AAG38506.1), Maize GST (P04907), hGSTA1-1 (NP_665683.1), hGSTM1-1 (P09488) and hGSTP1-1 (P09211), Red and Blue boxes represents key and lock residues in mammalian classes respectively. Arg 96 residue is marked with black dot.

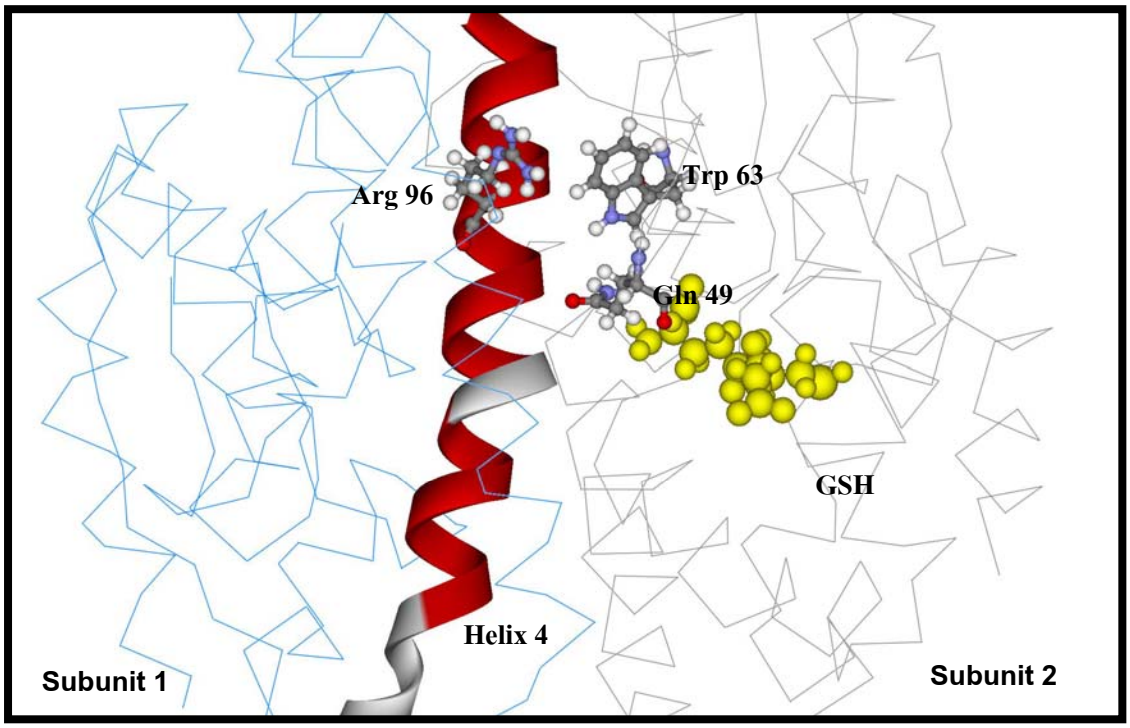

Figure 6: Proposed mode of communication between Arg96 and Trp63 residues: Backbones are drawn as α carbon-traces with the exception of the α4 that contains Arg96 of one subunit and the neighboring residues of the alternate subunit. Selected residues are drawn in a ball-and-stick representation, along with Arg96 and nearby interface forming residues. Glutathione is shown as yellow CPK module. The figure was created with DSviewerPro 5.0.

in modulating the substrate binding, catalysis and intersubunit communication (31). This residue is absent in mammalian classes. Based on the alignment of the maize GST and delta class GST; AdGSTD1-1 – AdGSTD4-4, the Asn 49 is also found in the delta class enzyme and equivalent to Asn 47 residue in AdGSTD3-3 (Figure 5). However, the residue functions in stability and folding. Mutation of this residue strongly affected the folding mechanism of the enzyme thereby making them incorrect folding. In the squid sigma class study (32), residues at the interface positions are more hydrophilic thereby predominating with polar interaction and made them stable in the monomeric state in equilibrium unfolding study suggesting the role of hydrophilic residues that would be stable when exposed to solvent. In contrast alpha, mu and pi classes, lack this form in the unfolding pathway. However, the unfolding study of AdGSTD3-3 still requires further studies.

For the explanation in changes of catalysis and substrate binding, Arg 96 mutation may affect the rearrangement of Trp 63 residue and indirectly affect Asn 47 and Gln 49 that are tightly packed in the active site region. This affect was firstly reported by Winayanuwattikun P. (18), mutation of Arg 66 can also affect Trp 63 and change the tertiary structure at the active site by changing the intrinsic fluorescence of the Arg66A. In addition, residues Asn 47, Pro 48 and Gln 49 are active site residues located in helix 2 which normally function by modulating the affinity of GSH binding and involve in intersubunit communication in hGSTP1 (33-35). Based on the results in Table 2, Gln49Ala mutant demonstrated an increased K_m toward GSH approximately 4-fold as found in other studies. In addition, mutation at position 63 also supported the effect of helix 2 purturbation by showing the decreasing binding affinity of GSH substrate.

Alternatively, mutations of residue 49 and 63 may perturb the flexibility of helix 2 thereby affecting the binding process of AdGSTD3-3.

For the effect on the stability of the enzyme, Trp 63 is located in β4 that help in stability and folding of GST enzyme in domain 1. The folding in this domain is initiated by interaction between β2 and β4 region (36). Mutation of residue at Trp 63 may affect the tertiary structure and reduce the half-life to 50%. Ihis also explains the reason of low protein yield obtained in Table 1 of Trp63Ala. The study suggested the role of interface residue of delta class GST that may be involved in the stability of the enzyme. The explanation for the modulation of substrate specificity, the $V_{max,}$ and the K_m appears to be due to structural perturbations that induce small changes in active site topology that affect binding and catalysis.

Conclusion

1. In this study, the interface residue Arg 96 of AdGSTD3-3 enzyme have been studied. Five mutants of AdGSTD3-3 at this positions were generated. In addition, five neighboring residues of Arg 96 were replaced with Ala residue.

2. The recombinant clones with single residue changes from the above were purified and characterized. The characterization results show that Arg 96 mutants possess differences in kinetic properties especially the K_m^{GSH}.

3. The majority of Arg 96 mutants were shown to be thermally more stable than the wild type enzyme indicating an important role for this residue in structural stabilization.

4. Arg 96 residue not only has a series of residue interaction in the intra subunit of the protein, it also affects the interaction with Trp 63 in the other subunit. The positional changes in Trp 63 would then influence the interaction with Gln 49 which is an active site residue in the other subunit.

Reference List

(1) Chareonviriyaphap T, Bangs MJ, Ratanatham S. Status of malaria in Thailand. Southeast Asian J Trop Med Public Health 2000; 31(2):225-237.

(2) Wilce MCJ, Parker MW. Structure and function of glutathione S-transferases. Biochim Biophys Acta 1994; 1205:1-18.

(3) Dulhunty A, Gage P, Curtis S, Chelvanayagam G, Board P. The glutathione transferase structural familyincludes a nuclear chloride channel and a ryanodine receptor calcium release channel modulator. J Biol Chem 2001; 276(5):3319-3323.

(4) Tchaikovskaya T, Fraifeld V, Urphanishvili T, Andorfer JH, Davies P, Listowsky I. Glutathione S-transferase hGSTM3 and ageing-associated neurodegeneration: relationship to Alzheimer's disease. Mech Ageing Dev 2005; 126(2):309-315.

(5) Udomsinprasert R, Bogoyevitch MA, Ketterman AJ. Reciprocal regulation of glutathione *S*-transferase spliceforms and the *Drosophila* c-Jun N-terminal Kinase pathway components. Biochem J 2004.

(6) Armstrong RN. Structure, catalytic mechanism, and evolution of the glutathione transferases. Chem Res Toxicol 1997; 10:2-18.

(7) Sawicki R, Singh SP, Mondal AK, Beneš H, Zimniak P. Cloning, expression and biochemical characterization of one Epsilon-class (GST-3) and ten Delta-class (GST-1) glutathione S-transferases from *Drosophila melanogaster*, and

identification of additional nine members of the Epsilon class. Biochem J 2003; 370:661-669.

(8) Sheehan D, Meade G, Foley VM, Dowd CA. Structure, function and evolution of glutathione transferases : implications for classification of non-mammalian members of an ancient enzyme superfamily. Biochem J 2001; 360:1-16.

(9) Board PG, Coggan M, Chelvanayagam G, Easteal S, Jermiin LS, Schulte GK et al. Identification, characterization, and crystal structure of the omega class glutathione transferases. J Biol Chem 2000; 275:24798-24806.

(10) Ji X, Von Rosenvinge EC, Johnson WW, Tomarev SI, Paitigorsky J, Armstrong RN et al. Three-dimensional structure, catalytic properties, and evolution of a sigma class glutathione transferase from squid, a progenitor of the lens S-crystallins of cephalopods. Biochemistry 1995; 34:5317-5328.

(11) Oakley AJ, Harnnoi T, Udomsinprasert R, Jirajaroenrat K, Ketterman AJ, Wilce MCJ. The crystal structures of glutathione S-transferases isozymes 1–3 and 1–4 from *Anopheles dirus* species B. Protein Science 2001; 10:2176-2185.

(12) Reinemer P, Dirr HW, Ladenstein R, Huber R, Lo Bello M, Federici G et al. Three-dimensional structure of class p glutathione S-transferase from human placenta in complex with S-hexylglutathione at 2.8 ล resolution. J Mol Biol 1992; 227:214-226.

(13) Reinemer P, Prade L, Hof P, Neuefeind T, Huber R, Zettl R et al. Three-dimenstional structure of glutathione S-transferase from *Arabidopsis thaliana* at 2.2 ล resolution: structural characterization of herbicide-conjugating plant

glutathione S-transferases and a novel active site architecture. J Mol Biol 1996; 255:289-309.

(14) Sinning I, Kleywegt GJ, Cowan SW, Reinemer P, Dirr HW, Huber R et al. Structure determination and refinement of human Alpha class glutathione transferase A1-1, and a comparison with the Mu and Pi class enzymes. J Mol Biol 1993; 232:192-212.

(15) Ding Y, Ortelli F, Rossiter LC, Hemingway J, Ranson H. The *Anopheles gambiae* glutathione transferase supergene family: annotation, phylogeny and expression profiles. BMC Genomics 2003; 4:35-50.

(16) Pongjaroenkit S, Jirajaroenrat K, Boonchauy C, Chanama U, Leetachewa S, Prapanthadara L et al. Genomic organization and putative promotors of highly conserved glutathione S-transferases originating by alternative splicing in *Anopheles dirus*. Insect Biochem Molec Biol 2001; 31(1):75-85.

(17) Jirajaroenrat K, Pongjaroenkit S, Krittanai C, Prapanthadara L, Ketterman AJ. Heterologous expression and characterization of alternatively spliced glutathione *S*-transferases from a single *Anopheles* gene. Insect Biochem Molec Biol 2001; 31:867-875.

(18) Winayanuwattikun P, Ketterman AJ. Catalytic and structural contributions for glutathione binding residues in a delta class glutathione S-transferase. Biochem J 2004; 382:751-757.

(19) Ketterman AJ, Prommeenate P, Boonchauy C, Chanama U, Leetachewa S, Promtet N et al. Single amino acid changes outside the active site significantly

affect activity of glutathione S-transferases. Insect Biochem Molec Biol 2001; 31(1):65-74.

(20) Park H-J, Lee K-S, Cho S-H, Kong K-H. Functional studies of cysteine residues in human glutathione *S*-transferase P1-1 by site-directed mutagenesis. Bull Korean Chem Soc 2001; 22(1):77-83.

(21) Sayed Y, Wallace LA, Dirr HW. The hydrophobic lock-and-key intersubunit motif of glutathione transferase A1-1: implications for catalysis, ligandin function and stability. FEBS Lett 2000; 465:169-172.

(22) Wallace LA, Burke J, Dirr HW. Domain-domain interface packing at conserved Trp-20 in class a glutathione transferase impacts on protein stability. Biochem Biophys Acta 2000; 1478:325-332.

(23) Xiao B, Singh SP, Nanduri B, Awasthi YC, Zimniak P, Ji X. Crystal structure of a murine glutathione S-transferase in complex with a glutathione conjugate of 4-hydroxynon-2-enal in one subunit and glutathione in the other: evidence of signaling across the dimer interface. Biochemistry 1999; 38:11887-11894.

(24) Wongtrakul J, Sramala I, Ketterman A. A non-active site residue, cysteine 69, of glutathione S-transferase adGSTD3-3 has a role in stability and catalytic function. Protein and Peptide Letters 2003; 10(4):375-385.

(25) Wongtrakul J, Udomsinprasert R, Ketterman A. Non-active site residues Cys69 and Asp150 affected the enzymatic 53 properties of glutathione *S*-transferase AdGSTD3-3. Insect Biochem Molec Biol 2003; 33(971):979.

(26) Wongtrakul J, Sramala I, Prapanthadara LA, Ketterman AJ. Intra-subunit residue interactions from the protein surface to the active site of glutathione S-

transferase AdGSTD3-3 impact on structure and enzyme properties. Insect Biochem Mol Biol 2005; 35(3):197-205.

(27) Jakoby WB, Habig WH. Glutathione transferases. In: Jakoby WB, editor. Enzymatic Basis of Detoxication Vol. 2. New York: Academic Press, 1980: 63-94.

(28) Hu Z, Ma B, Wolfson H, Nussinov R. Conservation of polar residues as hot spots at protein interfaces. Proteins 2000; 39:331-342.

(29) Hornby JAT, Codreanu SG, Armstrong RN, Dirr HW. Molecular recognition at the dimer interface of a class Mu glutathione transferase: Role of a hydrophobic interaction motif in dimer stability and protein function. Biochemistry 2002; 41(48):14238-14247.

(30) Stenberg G, Abdalla A-M, Mannervik B. Tyrosine 50 at the subunit interface of dimeric human glutathione transferase P1-1 is a structural key residue for modulating protein stability and catalytic function. Biochem Biophys Res Comm 2000; 271:59-63.

(31) Labrou NE, Mello LV, Clonis YD. The conserved Asn49 of maize glutathione *S*-transferase I modulates substrate binding, catalysis and intersubunit communication. Eur J Biochem 2001; 268:3950-3957.

(32) Stevens JM, Hornby JAT, Armstrong RN, Dirr HW. Class sigma glutathione transferase unfolds via a dimeric and a monomeric intermediate: Impact of subunit interface on conformational stability in the superfamily. Biochemistry 1998; 37:15534-15541.

(33) Lo Bello M, Nuccetelli M, Chiessi E, Lahm A, Mazzetti AP, Parker MW et al. Mutations of Gly to Ala in human glutathione transferase P1-1 affect helix 2 (G-Site) and induce positive cooperativity in the binding of glutathione. J Mol Biol 1998; 284:1717-1725.

(34) Stella L, Caccuri AM, Rosato N, Nicotra M, Lo Bello M, De Matteis F et al. Flexibility of helix 2 in the human glutathione transferase P1-1. Time-resolved fluorescence spectroscopy. J Biol Chem 1998; 273(36):23267-23273.

(35) Stella L, Nicotra M, Ricci G, Rosato N, Di Iorio EE. Molecular dynamics simulations of human glutathione transferase P1-1: analysis of the induced-fit mechanism by GSH binding. Proteins 1999; 37:1-9.

(36) Tasayco ML, Fuchs J, Yang X-M, Dyalram D, Georgescu RE. Interaction between two discontiguous chain segments from the b-sheet of *Escherichia coli* thioredoxin suggests an initiation site for folding. Biochemistry 2000; 39(35):10613-10618.

Output

1. The results obtained from this study has been published as indicated below;

Wontrakul J, Sramala I, Prapanthadara L and Ketterman AJ. Intra-subunit residue interactions from the protein surface to the active site of Glutathione S-transferase AdGSTD3-3 impact on structure and enzyme properties. Insect Biochem Mol Biol. 2005 35: 197-205.

2 Some parts of this work were presented in The Thailand Research Fund annual meeting at Karnchanaburi, 14-16 March 2005 as the poster presentation. **Wontrakul J**, Prapanthadara L and Ketterman AJ. Interface Residue, Arg 96, Of Glutathione S-transferase Modulates Enzyme Function.

Appendices

Available online at www.sciencedirect.com
SCIENCE DIRECT®
Insect Biochemistry and Molecular Biology 35 (2005) 197–205
Insect Biochemistry and Molecular Biology
www.elsevier.com/locate/ibmb

Intra-subunit residue interactions from the protein surface to the active site of glutathione S-transferase AdGSTD3–3 impact on structure and enzyme properties

Jeerang Wongtrakul[a], Issara Sramala[b], La-aied Prapanthadara[a], Albert J. Ketterman[b,*]

[a]*Research Institute for Health Sciences, Chiang Mai University, P.O. Box 80 CMU, Thailand 50200*
[b]*Institute of Molecular Biology & Genetics, Mahidol University, Salaya campus, 25/25 Putthamonthol Road 4, Salaya, Nakon Pathom 73170, Thailand*

Received 16 August 2004; received in revised form 12 November 2004; accepted 17 November 2004

Abstract

Structural residues are one of the major factors that modulate the catalytic specificity as well as having a role in stability of the glutathione S-transferases (GST). To understand how residues remote from the active site can affect enzymatic properties, four mutants, His144Ala, Val147Leu, Val147Ala and Arg96Ala, were generated. The selected residues appear to be in a putative intra-subunit interaction pathway from the exterior Asp150 to the active site Arg66 of AdGSTD3–3. The analysis of the four mutants suggested that the interaction formed between Asp150 and His144 is required for the packing of the hydrophobic core in domain 2. Mutations of both Asp150 and His144 impacted upon enzymatic properties. Two Val147 mutants also showed contribution to packing and support of the N-capping box motif by demonstrating shorter half-lives. The planar guanidinium of Arg96 is in a stacked geometry with the face of the aromatic ring of Phe140 in a cation-π interaction. The Arg96 also interacts with several other residues one of which, Asp100, is in the active site. These interactions restrict movement of the residues in this region and as the data demonstrates when Arg96 is changed have dramatic impact on stability and enzyme properties. These findings indicate the significance of the roles played by residue interactions which can cause conformational changes and thereby influence the catalytic activity and stability of an enzyme.

Keywords: Glutathione S-transferase; Structure; Molecular dynamics simulation; Enzyme specificity

1. Introduction

Glutathione S-transferases (EC 2.5.1.18; GSTs) are a family of enzymes involved in cellular detoxification by catalyzing the nucleophilic attack of glutathione (GSH) on the electrophilic center of a number of toxic compounds and xenobiotics such as insecticides (Booth et al., 1961). Besides their detoxification roles, GSTs are also involved in the modulation of signal transduction, ion channels and the storage of nitric oxide (Adler et al., 1999; Cho et al., 2001; Dulhunty et al., 2001; Lo Bello et al., 2001; Wang et al., 2001). Cytosolic GSTs have been grouped into at least 13 distinct classes, namely alpha, mu, pi, theta, sigma, kappa, omega, beta, phi, tau, zeta, delta and epsilon on the basis of immunological and structural properties (Sawicki et al., 2003; Sheehan et al., 2001). GSTs consist of identical or structurally related subunits. Each subunit, approximately 25 kDa, consists of two domains and contains an active site consisting of a G-site (GSH binding site) and an H-site (hydrophobic substrate binding site). The G-site is formed primarily by the N-terminal domain, which is structurally related to thioredoxin. The H-site is formed by the amino acids in the

Abbreviations: GST, glutathione S-transferase; GSH, glutathione; G-site, glutathione binding site; H-site, hydrophobic substrate binding site; CDNB, 1-chloro-2, 4-dinitrobenzene

*Corresponding author. Tel.: +66 2800 3624 8x1279; fax: +66 2441 9906.
E-mail addresses: frakt@mahidol.ac.th, albertketterman@yahoo.com (A.J. Ketterman).

0965-1748/$ - see front matter © 2004 Elsevier Ltd. All rights reserved.
doi:10.1016/j.ibmb.2004.11.003

region of the α4-helix to α8-helix. Whereas, the structure of the G-site is well conserved among GSTs, the H-site varies widely in different classes, leading to differences in substrate specificity (Armstrong, 1997). In addition, GSTs also possess a ligand binding site that is located in either part of the substrate binding site or at the dimer interface (Lyon and Atkins, 2002; Sayed et al., 2000).

Structural residues are one of the major factors that modulate the catalytic specificity as well as having a role in stability of the GSTs. Several of these residues have been identified as being located at the subunit interface, intra-domain interface and the N-terminus of helix 6 (Dragani et al., 1997; Luo et al., 2002; Xiao et al., 1999). In alpha class GST the interaction of Arg69 and Gln100 with the active site residue Arg15 appeared to control signaling across the subunits. A mutation of Arg69 to Ala resulted in a disruption of the signaling. Intra-subunit interactions have also been shown to be important in rGSTM1-1 where Arg77 in helix 3 forms inter-domain hydrogen bonds with Asp97 and Glu100 in helix 4 and with Tyr154 in helix 6, and thereby plays an important role in stabilizing the monomer (Luo et al., 2002). Recent work on an insect delta class GST (AdGSTD3–3) proposed that Asp150, located in the loop before helix 6, may contribute to the catalytic efficiency of the enzyme through an intra-subunit interaction with several residues in the interior of the protein that affects the active site (Wongtrakul et al., 2003b). Asp150 forms an ionic interaction with His144 (another residue in the loop between helix 5 and helix 6). As a result, the interaction appeared to stabilize the loop of residues 142–155 between helix 5 and 6. In addition, two conserved hydrophobic residues within the loop, Val147 and Ala148, also have van der Waal contact with neighboring residues in the hydrophobic core that support Arg96 in helix 4. Therefore, the movement of Arg96 residue may then influence Arg66 in the active site. The hypothesized residues positions and interactions are based upon observations of the available crystal structure for this protein (Protein Data Bank accession number 1JLV; (Oakley et al., 2001). To test this hypothesis, the roles of the three residues in the proposed pathway, His144, Val147 and Arg96, were studied further by means of site-directed mutagenesis. Two mutants, Asp150Ser and Asp150Tyr, demonstrated maximum changes in catalytic efficiency and the least stability (Wongtrakul et al., 2003b). Molecular dynamics simulations also were performed to characterize interactions in this region. Previously we have reported this delta class (insect class 1) GST enzyme as adGST 1–3, which had been named according to the insect GST nomenclature in use. However, to be in alignment with a proposed universal GST nomenclature we have renamed the enzyme AdGSTD3–3 (Chelvanayagam et al., 2001). Where the 'D' refers to the GST delta class and the subunit number remains the same since the subunits were enumerated as they were initially discovered. The double number, GSTD3–3 for example, signifies the enzyme is a homodimer.

2. Materials and methods

2.1. Site-directed mutagenesis

The plasmid pET3a containing AdGSTD3–3 coding sequence has previously been constructed (Jirajaroenrat et al., 2001). The construct was used as a DNA template in a PCR reaction according to Quick Change™ site-directed mutagenesis described by Stratagene. The following oligonucleotides R96A-f: 5′ CAGAAGCGCG-CCG TCGT**T**AACCAG**GCG**CTGTACTCGACATG 3′, H144A-f: 5′ CTGAACACCTTCCTGGACGGG**GC-CAAGTACGTGG**CG 3′, V147A-f: 5′ CTGGACGGG-CACAAGTAC**GCTGCAG**GCGACAGTCTGACG 3′ V147L-f: 5′ CTGGACGGGCACAAGTA**CTTAG**CG-GGCACAGTCTGACG 3′ were used as mutagenic primers for the mutants along the proposed pathway. The changed nucleotide residues are shown in bold type and the additional recognition sites for restriction endonucleases are underlined. The recombinant plasmids were randomly screened by restriction analysis then the nucleotide sequences of the plasmids carrying the mutations were verified by full-length sequencing in both directions using a Bigdye™ terminator cycle sequencing kit (Perkin Elmer).

2.2. Protein expression and purification

The protein expression and purification were carried out as previously described (Wongsantichon et al., 2003). After affinity purification the wild type and mutant enzymes were homogeneous as judged by SDS–PAGE. The protein concentration was determined by the method of Bradford using bovine serum albumin as the standard protein (Bradford, 1976).

2.3. Kinetic studies

The GST activity assays were performed as previously described (Prapanthadara et al., 1996). Thermal stability was measured as a function of time. All the wild type and mutant enzymes were incubated (0.1 mg/ml in 0.1 M potassium phosphate pH 6.5 containing 5 mM DTT and 1 mM EDTA) at 45 °C and aliquots were assayed for activity in the standard 1-chloro-2, 4-dinitrobenzene (CDNB) assay at different time-points.

2.4. Molecular dynamics simulation

Several one-nanosecond molecular dynamics trajectories of AdGSTD3–3 in complex with GSH were

generated. Gromac 3.0 (http://www.gromacs.org) with Gromacs force fields was used throughout the study. Initial coordinates of AdGSTD3–3 at 1.75 Å resolution (Protein Data Bank accession number 1 JLV) were from the X-ray crystal structure of the complex with GSH (Oakley et al., 2001). Residue Asp 150 was replaced with serine and tyrosine residues using Deepview Swiss-PdbViewer software (http://www.expasy.org/spdbv/). The file was then converted into (.GRO) format. The protein was immersed in a cubic box full of water molecules. Na^+ ions sufficient to neutralize the systems were added by replacing some of the water molecules to minimize the protein–ion electrostatic interaction. A temperature of 300 K was used for the minimization and molecular dynamics simulation. Molecular dynamics simulation was performed in an isobaric (NPT) ensemble. First a steepest descent energy minimization was performed without restraints to eliminate initial contacts of the protein atoms. Then a molecular dynamics simulation was performed with positional restraint on the protein atoms to let water and ions move freely in the system. Finally, an unrestrained molecular dynamics simulation was performed for 1 ns. The crystal structure and simulated structures were visualized either by DS ViewerPro 5.0 (Accelrys Inc) or Deepview Swiss-PdbViewer v3.5b4.

3. Results

The residues involved in the intra-subunit interaction characterized in this study are shown in Fig. 1. All the recombinant protein variants of the studied region were successfully expressed in *Escherichia.coli* and purified. Table 1 summarizes the kinetic constants for GSH-CDNB conjugation. Disruption of the ionic interaction by the substitution of His144 with Ala resulted in a 15% increase of k_{cat}, similar to the replacement of Asp150 with Ser, Tyr and Ala which ranged from 10% to 25% increase compared to the wild type. In addition, the K_m^{GSH} of His144Ala was approximately 1.3-fold larger than that of the wild type. It also possessed a similar K_m^{GSH} value compared to Asp150Ala mutant. In contrast, the His144 mutation scarcely affects the K_m^{CDNB} ,whereas all the Asp150 mutations significantly decreased the values. The Val147Ala mutant displayed a 1.5-fold decrease in catalytic efficiency with CDNB when compared with the wild type. An even greater effect with both GSH and CDNB was seen with Val147Leu. The replacement of Arg96 to Ala greatly affects the catalytic properties of AdGSTD3–3. For example, the k_{cat}, K_m^{GSH} and K_m^{CDNB} are 1.8-, 9.5- and 2.9-fold more than that of the wild type, respectively. In addition, the k_{cat}/K_m toward both GSH and CDNB substrates is 5.1-and 1.5-fold less than that of the wild type.

The specific activities of wild type AdGSTD3–3 and the variant enzymes were determined with five alternative substrates; 1-chloro-2, 4-dinitrobenzene, 1,2-dichloro-4-nitrobenzene (DCNB), 4-nitrobenzyl chloride, 4-nitrophenethyl bromide and ethacrynic acid. The substrates chosen have been reported to be preferred by different GST classes: CDNB—general substrate; DCNB—mu class; 4-nitrobenzyl chloride—rat theta

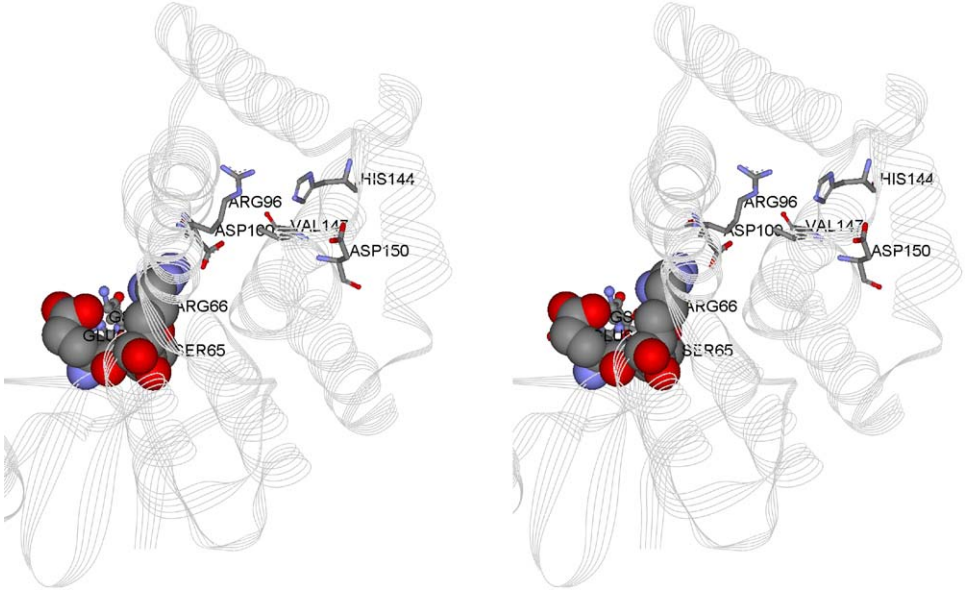

Fig. 1. Stereo view of the residues that are involved in a putative intra-subunit interaction in AdGSTD3–3. The figure shows a ribbon structure of one subunit of AdGSTD3–3 with several residues, His144, Asp150, Val147, Arg96 and Asp100 that appear to impact structurally upon Arg66. The active site residues, Glu64, Ser65 and Arg66 are shown in CPK. The substrate GSH, is shown in ball and stick form.

Table 1
Kinetic constants for the enzymes with residue changes along the proposed pathway of interaction

Enzymes	V_{max}	k_{cat}	GSH		CDNB	
			K_m	k_{cat}/K_m	K_m	k_{cat}/K_m
AdGSTD3-3[a]	63.6±6.2	25.2	0.29±0.03	86.9	0.13±0.01	194
Asp150Ser[a]	70.2±1.0	27.8	0.17±0.02	160	0.07±0.01	391
Asp150Tyr[a]	74.2±6.8	29.5	0.21±0.02	141	0.09±0.01	327
Asp150Ala[a]	80.2±7.0	31.7	0.33±0.02	96.7	0.08±0.02	382
His144Ala	73.7±3.3	29.1	0.37±0.06	79.5	0.14±0.01	205
Val147Ala	63.0±1.7	24.9	0.26±0.03	96.1	0.19±0.01	131
Val147Leu	54.4±1.2	21.6	0.34±0.04	63.6	0.20±0.04	105
Arg96Ala	118±7.0	46.8	2.75±0.12	17.0	0.38±0.06	125

Note: The units are: V_{max}: μmol/min/mg, K_m: mM, $k$cat: s^{-1}, k_{cat}/K_m: /mM/s. The data are mean±standard deviation from at least 3 independent experiments. The activity was measured in 0.1 M potassium phosphate, pH 6.5, 25–27 °C.
[a]From (Wongtrakul et al., 2003).

Table 2
Specific activity towards five different substrates for the enzymes with residue changes along the proposed pathway of interaction

Enzyme	CDNB (1 mM)	DCNB (1 mM)	4-nitrobenzyl chloride (0.1 mM)	4-nitrophenethyl bromide (0.1 mM)	Ethacrynic acid (0.2 mM)
AdGSTD3-3[a]	57.2±3.2	0.248±0.003	0.135±0.013	0.019±0.007	0.087±0.010
Asp150Ser[a]	64.7±5.5	0.249±0.005	0.142±0.009	0.070±0.008	0.126±0.016
Asp150Tyr[a]	63.9±3.7	0.289±0.003	0.173±0.020	0.067±0.013	0.100±0.016
Asp150Ala[a]	68.9±3.8	0.284±0.009	0.111±0.004	0.021±0.004	0.050±0.017
His144Ala	59.0±4.4	0.229±0.013	0.106±0.008	0.010±0.001	0.056±0.007
Val147Ala	68.8±2.0	0.243±0.005	0.135±0.018	0.018±0.004	0.101±0.014
Val147Leu	62.6±4.4	0.225±0.009	0.104±0.005	0.013±0.001	0.053±0.010
Arg96Ala	66.3±4.1	0.212±0.003	0.060±0.006	<0.005	0.045±0.006

The units are μmol/min/mg of protein. The data are mean±standard deviation from at least 3 independent experiments. The substrate concentration used were 1 mM CDNB, 1 mM DCNB (1,2-dichloro-4-nitrobenzene), 0.1 mM 4-nitrobenzyl chloride, 0.1 mM 4-nitrophenethyl bromide and 0.2 mM ethacrynic acid.
[a]From (Wongtrakul et al., 2003).

class; 4-nitrophenethyl bromide–human theta class and ethacrynic acid—pi class (Mannervik and Danielson, 1988; Hayes and Pulford, 1995). The results are compiled in Table 2. The single mutation that produced the most pronounced difference in specific activity is the Arg96Ala mutation, which decreased the specific activities for the substrates excluding CDNB. The Val147Ala mutation showed no changes in the specific activities for the same set of substrates. For His144Ala and Val147Leu, both mutations displayed small decreases in activities for the substrates. All the mutations showed little effect on the activity with the CDNB substrate.

An inhibition study of CDNB activity was performed using different compounds such as the hydrophobic substrates, pyrethroid insecticides and a GSH analog (Table 3). The residues studied showed only small effects for these compounds on the inhibition of CDNB activity. A result of interest was Arg96Ala which was still inhibited by 4-nitrophenethyl bromide although it no longer possessed any detectable activity for this as a substrate. It was observed that His144Ala, Val147Ala and Val147Leu mutants had a shorter half-life at 45 °C of approximately 50% compared to the wild type enzyme (Fig. 2). Therefore, both residues 144 and 147 significantly affect the packing of the hydrophobic core in domain 2. Surprisingly, the Arg96Ala was more stable with a half-life of approximately 187 min. Clearly the residue is involved in structural maintenance.

The models of Asp150 mutants from our previous results demonstrated conformational changes in domain 2 as shown by changes in several parameters such as helical dihedral angles and residue movement (Wongtrakul et al., 2003b). Therefore, molecular dynamics simulations of Asp150Ser and Asp150Tyr were performed to obtain a clearer understanding of the changes in the catalytic efficiency and the stability of the enzyme. The AdGSTD3-3 at position 150 was changed to Ser and Tyr residues. After the energy minimization and positional restraint, the system was simulated for 1000 ps. The fluctuation of the system was also monitored using the AdGSTD3–3 structure. The four control values were obtained by using the coordinates of AdGSTD3–3 after a 1000 ps MD simulation as starting coordinates, then performing four separate simulations

Table 3
Inhibition of CDNB activity of the enzymes with residue changes along the proposed pathway of interaction

Percent inhibition								
Enzyme	4-NBC 1 mM	CuOOH 2.5 mM	DCNB 1 mM	4-NPB 0.1 mM	Deltamethrin 0.01 mM	Permethrin 0.01 mM	EA 0.001 mM	S-hexyl 0.01 mM
Wild type	50.6±2.9	43.3±3.6	53.3±5.8	40.1±7.4	65.4±7.1	51.1±7.4	35.3±4.3	21.7±6.8
His144Ala	43.9±5.1	27.0±5.7	40.4±1.8	23.6±5.8	44.2±8.8	38.8±8.0	32.7±5.1	23.0±3.8
Val147Ala	40.8±7.5	50.6±2.0	42.4±4.2	19.5±7.3	59.5±2.5	53.1±7.0	27.8±2.6	10.8±4.4
Val147Leu	47.9±3.0	41.5±2.6	54.3±6.3	31.4±5.8	66.1±3.6	49.0±2.3	23.0±2.8	24.2±6.4
Arg96Ala	30.8±8.0	48.1±5.0	35.9±4.2	27.3±4.1	88.6±3.4	65.5±8.6	29.1±8.1	14.7±1.4

The data are mean±standard deviation for at least 3 independent experiments. Inhibition assays were performed using standard GST assay in the presence of 4-NBC, 4-nitrobenzyl chloride; CuOOH, cumene hydroperoxide; DCNB, 1,2-dichloro-4-nitrobenzene; 4-NPB, 4-nitrophenethyl bromide; deltamethrin, permethrin; EA, ethacrynic acid and S-hexyl glutathione.

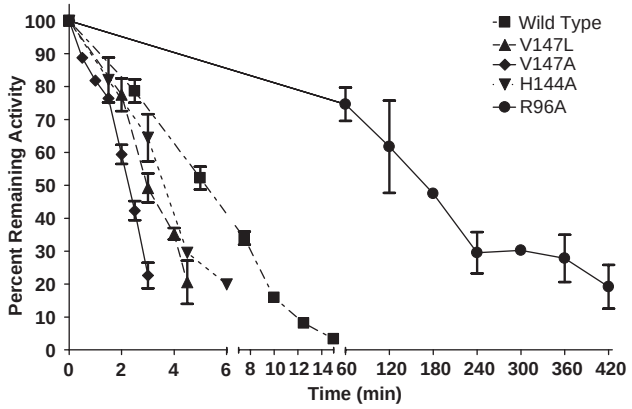

Fig. 2. Half-life time course at 45° for the enzymes with residue changes along the proposed pathway of interaction. Data plotted are means±standard deviations for three independent experiments.

for 200 ps with four different random seed numbers. Then the four sets of values were averaged and shown in Table 4.

The root mean square deviation (RMSD) indicates the difference between the protein structures obtained from the simulation and the original crystal structure. The RMSD were calculated from the alpha carbons of each GST peptide backbone. All of the simulations of wild type, Asp150Ser and Asp150Tyr reached a structural equilibrium after approximately 500 ps. All the simulations are characterized by a small deviation from the crystal structure, with an RMSD value of 0.8–1.6 Å over the time 500–1000 ps (Table 4). The radius of gyration which reflects the evolution of the overall shape of the protein was analyzed. For each of the simulations, the protein reached a structural equilibrium at similar values of the radius of gyration, very close to the value for the native state (approximately 20 Å). The total potential, electrostatic and van der Waals energies of wild type, Asp150Ser and Asp150Tyr showed similar fluctuations compared to the four controls. It was found that helix 2 and several loops that link GST helices showed a high mobility. This result was observed with a study in pi class where helix 2 was found to undergo extensive movement (Stella et al., 1999). Center of gravity analysis of our simulations shows changes in the structures do occur. This parameter measures the movement of the center of mass of the dimeric GST. It was found that the locations of Asp150 residue relative to the center of gravity in wild type and Asp150Tyr are similar at 0 and 1000 ps time points. Interestingly, Asp150Ser demonstrated different coordinates suggesting that it had different conformations at 0 and 1000 ps. The structural coordinates of the time point that showed maximum changes in center of gravity of Asp150Ser was generated and superimposed with the structure of the wild type at 1000 ps. It was found that the alpha carbon backbone of Asp150, Val147 and Val148 were shifted approximately 3 and 1.5 Å, respectively. In addition, the loop before helix 6 also faces the opposite direction compared to the wild type (Fig. 3). In the wild type protein, interaction between His144 and Asp150 appeared to be preserved in the MD simulation and even strengthened with an increased dipole–dipole interaction from His144 to the Asp150 backbone carbonyl oxygen (Fig. 3). In the mutant proteins the possible hydrogen bond formation from His144 to the O atom of the hydroxyl group of serine or tyrosine was not observed possibly due to packing rearrangements. In the simulation the distance was sometimes up to 7.28 Å from the His 144 to OH of Serine (Asp150Ser mutant) or 6.98 Å from the His 144 to OH of Tyr (Asp150Tyr mutant). Therefore, the results from the simulations support the proposed pathway.

4. Discussion

Characterization of Asp150 mutant enzymes from our previous work demonstrated that the mutation appeared to affect a sensitive region of the tertiary

Table 4
Analysis of the 1000 ps molecular dynamics simulations of the AdGSTD3-3 Asp-150 mutants

Parameters	Control	AdGSTD3-3	Asp150Ser	Asp150Tyr
Total energy	(−715306)–(−711620)	(−716836)–(−713671)	(−715379)–(−712271)	(−715602)–(−712129)
RMSD	0.827–1.309	1.092–1.586	1.003–1.496	0.917–1.307
Radius of gyration	20.179–20.5707	20.1483–20.5125	19.9965–20.33	20.0664–20.3439
Electrostatic energy	(−290.895)–(−55.26)	(−297.438)–(−97.6813)	(−186.964)–(−59.5189)	(−193.972)–(−53.3244)
Van der Waals energy	(−144.053)–(−54.368)	(−138.135)–(−50.1937)	(−136.97)–(−58.1716)	(−168.352)–(−86.9131)
Center of gravity (Cg)		(*X*, *Y*, *Z*)	(*X*, *Y*, *Z*)	(*X*, *Y*, *Z*)
Position changes of residue 150 relative to the Cg at 0 and 1000 ps		0 ps: 7.200, −10.890, 19.854 1000 ps: −0.0357, −14.348, 17.156	0 ps: −6.294, −11.370, 17.850 1000 ps: 1.258, −6.041, 21.229	0 ps: −5.389, −11.006, 19.102 1000 ps: −5.235, −12.744, 17.765
Maximum changes in Cg compared with the wild type			*X* = 5.8 Å (*T* = 673 ps) *Y* = 9.6 Å (*T* = 940 ps) *Z* = 6.1 Å (*T* = 937 ps)	*X* = 7.6 Å (*T* = 855 ps) *Y* = 3.6 Å (*T* = 781 ps) *Z* = 4.6 Å (*T* = 972 ps)

The units are: total energy: kJ/mol, RMSD: Å, radius of gyration: Å, electrostatic energy and Van der Waals energy: kJ/mol.

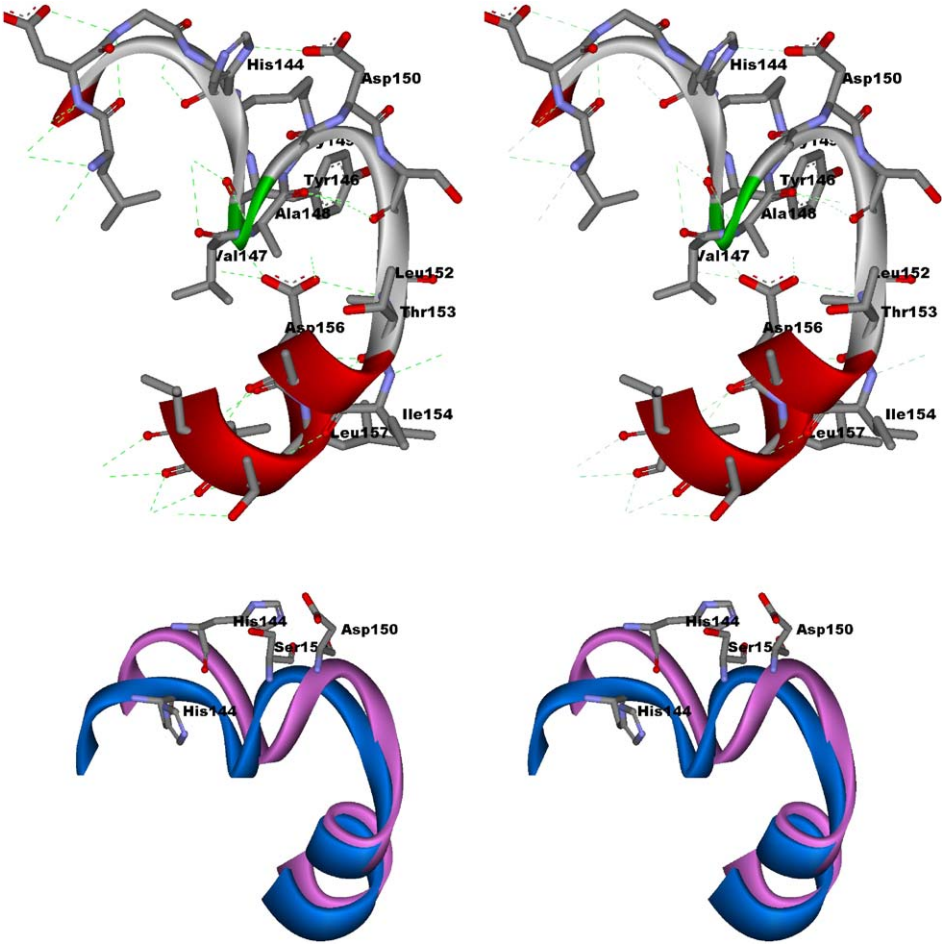

Fig. 3. Stereo view of the interhelical loop region in AdGSTD3–3. The top panel shows the N-capping box and hydrophobic staple motifs in AdGSTD3–3. H-bonds are shown as green dashed lines. The bottom panel shows the superimposition between Asp150Ser (blue) and wild type AdGSTD3–3 (purple) using the time point that showed maximum changes in the center of gravity compared with the wild type at 1000 ps.

structure resulting in changes in substrate specificity and stability (Wongtrakul et al., 2003b). In addition differing conformational changes were observed from Asp150 static models, e.g. dihedral angles of the helices, residue movements, etc. It was proposed that the mutation would affect neighboring residues that support two

important structural motifs, the N-capping box and the hydrophobic staple motif located in the loop before helix 6. Both motifs play a major role in the folding and stability of GSTs (Stenberg et al., 2000; Dragani et al., 1997; Cocco et al., 2001; Aceto et al., 1997). Therefore, the neighboring residue position Val147 was further studied after changing it to Ala and Leu. It was found that the mutations do affect the stability and catalytic activity of AdGSTD3–3 which support the hypothesis. Several studies have demonstrated that a mutation of a residue near an N-capping box decreases the stability of the GST. In GSTP1-1, Gly146 (Gly149 equivalent residue in AdGSTD3–3) which is a conserved residue found in all GSTs was shown to support the stability and refolding. This residue is located in a bend of the long loop before helix 6 with no specific contact with other parts of the molecule but only with neighboring residues that support the N-capping box motif. The mutation of Gly146 to Val lead to a substantial change of the backbone conformation (Kong et al., 2003). In addition, a Phe151Leu study in pi class also demonstrated a shorter half-life at 50 °C (Lin et al., 2003). Phe151 (Ile154 equivalent residue in AdGSTD3–3) is located at the N-terminus of helix 6. An analysis of tertiary structure suggested that the mutation produced a cavity in the core and destabilized the structure. Therefore, our study provides additional evidence of other neighboring residues that affect the N-capping box motif which leads to activity and stability changes in the enzyme.

In addition, two pathways were proposed, an intra- and an inter-subunit route of Asp150 residue interaction to the active site (Wongtrakul et al., 2003b).This study mainly focused on the intra-subunit interaction. Mutations of positions His144Ala, Val147Ala and Val147Leu between Asp150 and the catalytic residues in the active site were generated. The variant proteins all had shorter half-lives compared to the wild type enzyme of approximately 50%. The ionic interaction between Asp150 and His144 is required for the packing of the hydrophobic core in domain 2. Disruption of this ionic interaction formed by both residues made the loop before helix 6 more flexible. The residues on the loop would therefore pack in the hydrophobic core with greater movement compared to the wild type thereby giving the His144Ala protein a shorter half-life at 45 °C. Residue 147 is positioned in the hydrophobic core of domain 2 and contributes to packing so that the Val147Leu showed a slight variation in structure demonstrating a change in the stability and substrate activity when compared to the wild type. In addition, a decrease in core residue volume with Ala substitution also lead to losses in hydrophobic stabilization and favorable van der Waals interactions that occur as a result of the tighter packing in the core. Val147Ala possessed a shorter half-life compared to Val147Leu suggesting that the reduction of the size and hydrophobicity of the interior side-chain resulted in creating internal cavities thereby reducing the stability of the enzyme. Val147 and Ala148 appear to be conserved hydrophobic residues found in delta class GSTs e.g. Ala148 in *L. cuprina* and Ala148, Ala149 in *D. melanogaster*. Both residues are also conserved across AdGST isoenzymes, Ala147 and Ala148 in AdGSTD1-1, Val151 and Ala152 in AdGSTD2-2, Val155 and Ala156 in AdGSTD4-4. Val147 is equivalent to Ile144 and Leu148 in pi and alpha class, respectively. This residue was reported to have an important role in the stability of the final structure of the protein (Cocco et al., 2001; Dragani et al., 1997). In AdGSTD3–3, the amide NH of Val147 directly formed a hydrogen bond with Asp156 which is the N-capping box residue. This interaction is specific and required for stabilization of the long loop preceding helix 6 which is strictly conserved in GST classes (Aceto et al., 1997).

For the Arg96Ala enzyme, the mutation dramatically increased the stability of the enzyme to 187 min. The effect may be due to residue interactions at the subunit interface. However, the crystal structure of AdGSTD3–3 shows the main chain of Arg96 interacts with residues near the active site in its own subunit to support the active site structure. The amino side chain of Arg96 is in close contact, 3.6 Å, with the aromatic ring of Phe140 in helix 5, in a cation-π interaction (Fig. 4). The planar guanidinium of Arg is in a parallel or stacked geometry with the face of the aromatic ring. In addition, strengthening this geometry the Arg side chain NE atom hydrogen bonds to the carbonyl of Val147 which thus yields an energetically favorable configuration (Ma and Dougherty, 1997). The Arg96 also interacts with several other residues one of which, Asp100, is in the active site (Fig. 4). These interactions with Arg96 would restrict movement of the residues in this region and as the data demonstrates, when Arg96 is changed, yield different obtainable conformations that impact on stability and enzyme properties.

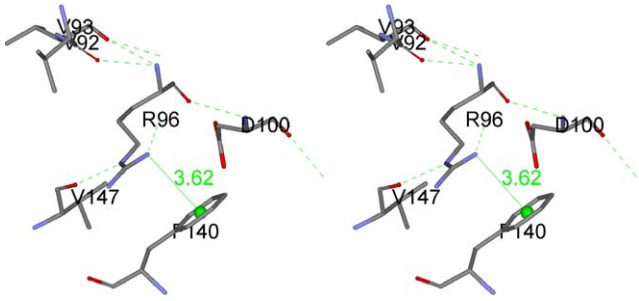

Fig. 4. Stereo view of residues interacting with Arg96. The dotted lines represent hydrogen bonds. The planar guanidinium of Arg96 is shown stacked with the face of the aromatic ring of Phe140. The sphere is the centroid of the benzene ring of Phe140 with the distance to the NH1 atom of Arg96 shown.

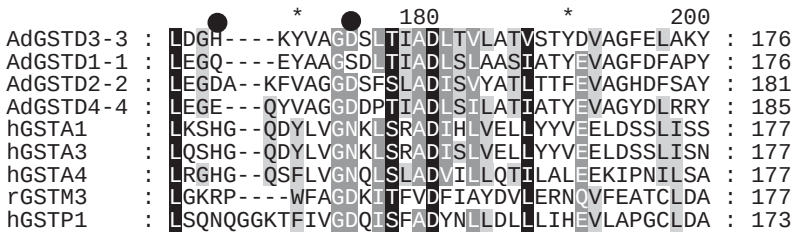

Fig. 5. Alignment of topologically equivalent amino acid residues of GSTs from different classes. Residue numbering for each sequence is shown at the right. Black, dark gray and light gray shadings represent 100%, 80% and 60% sequence similarity respectively. The sequences have the following Genbank accession numbers. AdGSTD3–3 (AAG38505.1), AdGSTD1-1 (AF273041_1), AdGSTD2-2 (AAG38504.1), AdGSTD4-4 (AAG38506.1), hGSTA1 (P08263), hGSTA3 (Q16772), hGSTA4 (AAD27704), rGSTM3 (P08009), hGSTP1 (P09211). His 144 and Asp 150 residues of AdGSTD3–3 are marked as black dots.

Based on the results from molecular dynamics simulations, the location of Asp150 relative to the center of gravity was changed during the simulation. The loop before helix 6 also faced a different direction compared to the wild type structure. In addition, Val147 and Ala148 had a slight movement in the alpha carbon backbone. The results from the simulations therefore support the static models (Wongtrakul et al., 2003a) by demonstrating a different conformation at the same position which is in the domain 2 region located adjacent to both the N-capping box and hydrophobic staple motifs.

An alignment of the topologically equivalent region of several classes of GSTs shows that both His144 and Asp150 are not widely conserved (Fig. 5). However, examination of the crystal structures for these proteins at the equivalent positions in the tertiary structure show there are residues present that form hydrogen bonds across the random coil loop to stabilize it. For example, in the delta GST AdGSTD4-4 (formerly AdGST1-4) Glu152 hydrogen bonds to the backbone nitrogen of Gly158, whereas in human pi GST the Asn136 side chain hydrogen bonds to the carbonyl backbone oxygen of both Phe142 and Gly145. In human alpha GST1-1 multiple hydrogen bonds form across the equivalent loop region from His143 to the carbonyl oxygen of Tyr147, the backbone nitrogen of Asp146 to the oxygen of the side chain of Asn151 and the side chain oxygen OD1 of Asp157 to the backbone nitrogen of Leu148. Therefore, although the residues in the region vary, this preserved functional stabilization of the random coil loop suggests relatively important structural contributions from the loop need to be maintained.

In the present study, the effects of residue interaction can be detected at every mutation in the proposed pathway as assessed by changes in kinetic properties and the stability. Mutations of both Asp150 and His144 impacted upon enzymatic properties. Differences in kinetic parameters were also detected when Val147 was mutated to Ala and Leu. The effect was greater when Arg96 was replaced with Ala. The mutant showed marked differences in every kinetic parameter. Therefore, the pathway of residue interaction in AdGSTD3–3 is likely to occur by Asp150 influencing specificity and catalysis through affects on the active site Arg66 from Arg96 with contributions from His144 and Val147.

In summary, the results described here show that the ionic interaction between Asp150 and His144 impacts on catalysis of AdGSTD3–3 via intra-subunit interactions of multiple residues. In addition, a change of Asp150 and the alterations in volume of the hydrophobic core may bring about secondary effects altering the stability of the enzyme by influencing the N-capping box region. These findings indicate the significance of the roles played by residue interactions which can cause conformational changes and thereby influence the catalytic activity and stability of an enzyme.

Acknowledgements

This work was supported by the Thailand Research Fund (TRF) to J.W.

References

Aceto, A., Dragani, B., Melino, S., Allocati, N., Masulli, M., Di Ilio, C., Petruzzelli, R., 1997. Identification of an N-capping box that affects the α6-helix propensity in glutathione S-transferase superfamily proteins: a role for an invariant aspartic residue. Biochem. J. 322, 229–234.

Adler, V., Yin, Z., Fuchs, S.Y., Benezra, M., Rosario, L., Tew, K.D., Pincus, M.R., Sardana, M., Henderson, C.J., Wolf, C.R., Davis, R.J., Ronai, Z., 1999. Regulation of JNK signaling by GSTp. EMBO J 18, 1321–1334.

Armstrong, R.N., 1997. Structure, catalytic mechanism, and evolution of the glutathione transferases. Chem. Res. Toxicol. 10, 2–18.

Booth, J., Boyland, E., Sims, P., 1961. An enzyme from rat liver catalysing conjugations with glutathione. Biochem. J. 79, 516–524.

Bradford, M.M., 1976. A rapid and sensitive method for the quantitation of microgram quantities of protein utilizing the principle of proteindye binding. Anal. Biochem. 72, 248–254.

Chelvanayagam, G., Parker, M.W., Board, P.G., 2001. Fly fishing for GSTs: a unified nomenclature for mammalian and insect glutathione transferases. Chem. Biol. Interact. 133, 256–260.

Cho, S.-G., Lee, Y.H., Park, H.-S., Ryoo, K., Kang, K.W., Park, J., Eom, S.-J., Kim, M.J., Chang, T.-S., Choi, S.-Y., Shim, J., Kim,

Y., Dong, M.-S., Lee, M.-J., Kim, S.G., Ichijo, H., Choi, E.-J., 2001. Glutathione S-transferase Mu modulates the stress-activated signals by suppressing apoptosis signal-regulating kinase 1. J. Biol. Chem. 276, 12749–12755.

Cocco, R., Stenberg, G., Dragani, B., Principe, D.R., Paludi, D., Mannervik, B., Aceto, A., 2001. The folding and stability of human alpha class glutathione transferase A1-1 depend on distinct roles of a conserved N-capping box and hydrophobic staple motif. J. Biol. Chem. 276, 32177–32183.

Dragani, B., Stenberg, G., Melino, S., Petruzzelli, R., Mannervik, B., Aceto, A., 1997. The conserved N-capping box in the hydrophobic core of glutathione S-transferase P1–1 is essential for refolding. Identification of a buried and conserved hydrogen bond important for protein stability. J. Biol. Chem. 272, 25518–25523.

Dulhunty, A., Gage, P., Curtis, S., Chelvanayagam, G., Board, P., 2001. The glutathione transferase structural family includes a nuclear chloride channel and a ryanodine receptor calcium release channel modulator. J. Biol. Chem. 276, 3319–3323.

Hayes, J.D., Pulford, D.J., 1995. The glutathione S-transferase supergene family: regulation of GST and the contribution of the isoenzymes to cancer chemoprotection and drug resistance. CRC Crit. Rev. Biochem. Molec. Biol. 30, 445–600.

Jirajaroenrat, K., Pongjaroenkit, S., Krittanai, C., Prapanthadara, L., Ketterman, A.J., 2001. Heterologous expression and characterization of alternatively spliced glutathione S-transferases from a single *Anopheles* gene. Insect Biochem. Molec. Biol. 31, 867–875.

Kong, G.K.W., Polekhina, G., McKinstry, W.J., Parker, M.W., Dragani, B., Aceto, A., Paludi, D., Principe, D.R., Mannervik, B., Stenberg, G., 2003. Contribution of glycine 146 to a conserved folding module affecting stability and refolding of human glutathione transferase P1-1. J. Biol. Chem. 278, 1291–1302.

Lin, H.J., Johansson, A.-S., Stenberg, G., Materi, A.M., Park, J.M., Dai, A., Zhou, H., Gim, J.S.Y., Kau, I.H., Hardy, S.I., Parker, M.W., Mannervik, B., 2003. Naturally occurring Phe151Leu substitution near a conserved folding module lowers stability of glutathione transferase P1–1. Biochim. Biophys. Acta 1649, 16–23.

Lo Bello, M., Nuccetelli, M., Caccuri, A.M., Stella, L., Parker, M.W., Rossjohn, J., McKinstry, W.J., Mozzi, A.F., Federici, G., Polizio, F., Pedersen, J.Z., Ricci, G., 2001. Human glutathione transferase P1-1 and nitric oxide carriers: a new role for an old enzyme. J. Biol. Chem. 276, 42138–42145.

Luo, J.-K., Hornby, J.A.T., Wallace, L.A., Chen, J., Armstrong, R.N., Dirr, H.W., 2002. Impact of domain interchange on conformational stability and equilibrium folding of chimeric class μ glutathione transferases. Protein Sci. 11, 2208–2217.

Lyon, R.P., Atkins, W.M., 2002. Kinetic characterization of native and cysteine 112-modified glutathione S-transferase A1-1: reassessment of nonsubstrate ligand binding. Biochemistry 41, 10920–10927.

Ma, J.C., Dougherty, D.A., 1997. The cation-p interaction. Chem. Rev. 97, 1303–1324.

Mannervik, B., Danielson, U.H., 1988. Glutathione transferases—structure and catalytic activity. CRC Crit. Rev. Biochem. 23, 283–337.

Oakley, A.J., Harnnoi, T., Udomsinprasert, R., Jirajaroenrat, K., Ketterman, A.J., Wilce, M.C.J., 2001. The crystal structures of glutathione S-transferases isozymes 1–3 and 1–4 from *Anopheles dirus* species B. Protein Sci. 10, 2176–2185.

Prapanthadara, L., Koottathep, S., Promtet, N., Hemingway, J., Ketterman, A.J., 1996. Purification and characterization of a major glutathione S-transferase from the mosquito *Anopheles dirus* (species B). Insect Biochem. Molec. Biol. 26, 277–285.

Sawicki, R., Singh, S.P., Mondal, A.K., Beneš, H., Zimniak, P., 2003. Cloning, expression and biochemical characterization of one epsilon-class (GST-3) and ten delta-class (GST-1) glutathione S-transferases from *Drosophila melanogaster*, and identification of additional nine members of the epsilon class. Biochem. J. 370, 661–669.

Sayed, Y., Wallace, L.A., Dirr, H.W., 2000. The hydrophobic lock-and-key intersubunit motif of glutathione transferase A1-1: implications for catalysis, ligandin function and stability. FEBS Lett. 465, 169–172.

Sheehan, D., Meade, G., Foley, V.M., Dowd, C.A., 2001. Structure, function and evolution of glutathione transferases: implications for classification of non-mammalian members of an ancient enzyme superfamily. Biochem. J. 360, 1–16.

Stella, L., Nicotra, M., Ricci, G., Rosato, N., Di Iorio, E.E., 1999. Molecular dynamics simulations of human glutathione transferase P1-1: analysis of the induced-fit mechanism by GSH binding. Proteins 37, 1–9.

Stenberg, G., Dragani, B., Cocco, R., Mannervik, B., Aceto, A., 2000. A conserved "hydrophobic staple motif" plays a crucial role in the refolding of human glutathione transferase P1-1. J. Biol. Chem. 275, 10421–10428.

Wang, T., Arifoglu, P., Ronai, Z., Tew, K.D., 2001. Glutathione *S*-transferase P1-1 (GSTP1-1) inhibits c-Jun N-terminal kinase (JNK1) signaling through interaction with the C terminus. J. Biol. Chem. 276, 20999–21003.

Wongsantichon, J., Harnnoi, T., Ketterman, A.J., 2003. A sensitive core region in the structure of glutathione S-transferases. Biochem. J. 373, 759–765.

Wongtrakul, J., Sramala, I., Ketterman, A., 2003a. A non-active site residue, cysteine 69, of glutathione S-transferase adGSTD3–3 has a role in stability and catalytic function. Protein Peptide Lett. 10, 375–385.

Wongtrakul, J., Udomsinprasert, R., Ketterman, A., 2003b. Non-active site residues Cys69 and Asp150 affected the enzymatic 53 properties of glutathione *S*-transferase AdGSTD3–3. Insect Biochem. Molec. Biol. 33, 979.

Xiao, B., Singh, S.P., Nanduri, B., Awasthi, Y.C., Zimniak, P., Ji, X., 1999. Crystal structure of a murine glutathione S-transferase in complex with a glutathione conjugate of 4-hydroxynon-2-enal in one subunit and glutathione in the other: evidence of signaling across the dimer interface. Biochemistry 38, 11887–11894.

Interface Residue, Arg 96, Of Glutathione S-transferase Modulates Enzyme Function

Jeerang Wongtrakul[a] , La-aied Prapanthadara[a] and Albert J. Ketterman[b]
[a]Research Institute for Health Sciences(RIHES), Chiang Mai University, P.O.BOX 80 CMU, Chiang Mai, 50200,
e-mail: jwongtrakul@yahoo.com, inhso001@chiangmai.ac.th
[b]Institute of Molecular Biology and Genetics, Mahidol University, Nakonpathom, 73170, e-mail frakt@mahidol.ac.th

Abstract:

Glutathione S-transferases are multifunctional enzymes that have a major role in detoxification of physiological substances as well as xenobiotic compounds. A subunit interface residue, Arg 96 of a homodimeric class delta glutathione transferase, AdGSTD3-3, was characterized by enzyme activity and stability assays. Five mutants at amino acid 96 were generated as well as five neighboring residue mutants of the amino acid position 96. The results indicated that Arg 96 is an important residue in this region because either eliminating, reversing the charge or changing its neighboring residues results in varied kinetic effects on CDNB substrate and stronger effects on GSH substrate e.g. V_{max}, K_m and K_{cat}/K_m. In addition there is a relationship between the amino acid property in position 96 and thermal stability of the AdGSTD3-3, where more non-polar and uncharged residues in this position generate a thermally more stable enzyme. The results suggested that Arg 96 residue at the interface affects the interaction with Trp 63 in the other subunit. The positional changes in Trp 63 would then influence the interaction with Gln 49 which is an active site residue in the other subunit and modulate the catalytic activity of AdGSTD3-3 due to structural perturbations that induce small changes in active site topology that affect binding and catalysis.

Introduction:

Glutathione S-transferases (GSTs) (E.C. 2.5.1.18) are dimeric cellular detoxification enzymes that catalyze the conjugation of glutathione to endogenous metabolites and a wide range of xenobiotics (Armstrong, R.N.1997). GSTs, have been categorized into at least 12 classes (Sheehan, D. 2001). Based on the tertiary structure of AdGSTD3-3, Arg 96 interface residue is of particular interest. It is located in helix 4. The main chain of this residue supports the structure of active site residues 64-66 in helix 3 whereas the side chain of Arg 96 has van der Waal contact with Phe 140, which is a residue in helix 5 in the same subunit and Trp 63 that is located in β4 of the other subunit. Arg 96 is also close to residue 47-49, Asn 47, Pro 48 and Gln 49 that are near by the GSH binding site in the other subunit (Figure 1). Arg 96 was found to participate in the intra subunit pathway of residue interaction from Asp 150, located in the loop before helix 6, to Arg 66, which is an active site residue (Wongtrakul, J. et al. in press). In addition, a mutation of Arg96 to Ala significantly increased the half-life of the enzyme to approximately 3 hours at 45°C and increased K_m toward GSH substrates approximately 9.5-fold. This work therefore aimed to further study the role of this important interface residue by replacement with different amino acids to assess the contribution of the residue toward the catalytic function as well as protein conformational stability. In addition, neighboring residues of Arg 96 were replaced with Ala e.g. Trp 63, Phe 140, Asn 47, Pro 48 and Gln 49.

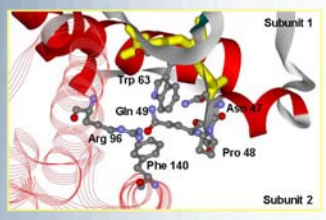

Figure1: Local structure around Arg 96 of AdGSTD3-3. The side chain of Arg 96 in one subunit of the protein, shown in a ball-and-stick representation, interacts with Phe 140 in its own subunit. In addition Arg 96 also interacts with Trp 63 in the other subunit. Both Phe 140 and Trp 63 are located close to Asn 47, Pro 48 and Gln 49 residues which are in the active site in the other subunit. The subunits are distinguished by pattern (line and flat ribbon). The active-site ligands are shown as stick representations.

Methods:

Construction of mutants: The DNA encoding AdGSTD3-3 in pET3a was used as a template in the mutagenesis procedure (1). The mutants AdGSTD3-3 were constructed using PCR with the QuickChangeTM Site-Directed Mutagenesis Kit (Stratagene). Clones with the required mutation were identified by restriction digest of the plasmids, and confirmed by full-length sequencing in both directions. Homogeneous enzyme preparations were obtained by heterologous expression and purification with GSTrap affinity chromatography.

Methods: (continued)

Characterization of the expressed enzymes: K_m and V_{max} for 1-chloro-2, 4-dinitrobenzene (CDNB) and GSH were determined using Graphad Prism 2.01 Software. Specific activities toward several GST substrates were determined spectrophotometrically, using the appropriate pH and λ max. Percent inhibition studies were performed using the standard GST assay conditions (10mM GSH and 1mM CDNB) in the presence and absence of the various compounds. In the thermal stability assay, the enzyme was incubated at 50°C. Aliquots were assayed for activity at different time points.

Results:

Enzyme	Protein yield (%)	V_{max} CDNB at 10 mM GSH	k_{cat}	CDNB K_m	CDNB k_{cat}/K_m
AdGSTD3-3	31	29.3 ± 0.2	11.6	0.13 ± 0.02	89.2
Arg96Lys	16	26.3 ± 1.8	10.4	0.12 ± 0.02	86.7
Arg96Phe	25	47.2 ± 1.8	18.7	0.16 ± 0.01	116
Arg96Tyr	30	39.7 ± 3.3	15.7	0.16 ± 0.02	98.1
Arg96Leu	37	52.7 ± 2.6	20.8	0.25 ± 0.04	83.2
Arg96Ala	19	24.7 ± 1.1	9.75	0.50 ± 0.04	19.5
Arg96Glu	7	54.9 ± 4.1	21.7	0.24 ± 0.03	90.4
Pro48Ala	24	22.7 ± 1.0	8.99	0.15 ± 0.04	59.9
Gln49Ala	31	53.8 ± 1.1	21.3	0.42 ± 0.04	50.7
Trp63Ala	2	9.20 ± 0.1	3.63	0.07 ± 0.02	50.4
Phe140Ala	8	27.9 ± 2.7	11.0	0.30 ± 0.02	36.7

Table 1: Kinetic constants for Arg 96 and its mutants toward CDNB substrate. The units are: V_{max}: μmole/min/mg, Km: mM, k_{cat}: s-1, k_{cat}/K_m: mM^{-1} s^{-1}. The data are mean ± standard deviation from at least 3 independent experiments.

Enzyme	V_{max} GSH at 1 mM CDNB	k_{cat}	GSH K_m	GSH k_{cat}/K_m
AdGSTD3-3	19.0 ± 1.8	7.5	0.20 ± 0.06	37.5
Arg96Lys	23.3 ± 1.5	9.2	0.44 ± 0.05	20.9
Arg96Phe	59.4 ± 1.2	23.5	0.61 ± 0.04	38.5
Arg96Tyr	42.0 ± 2.9	16.6	0.63 ± 0.04	26.3
Arg96Leu	38.6 ± 4.3	15.3	0.60 ± 0.06	25.5
Arg96Ala	30.3 ± 3.0	12.0	4.1 ± 0.50	2.93
Arg96Glu	46.1 ± 2.8	18.2	0.49 ± 0.02	37.1
Pro48Ala	23.6 ± 1.8	9.3	0.33 ± 0.04	28.2
Gln49Ala	43.0 ± 3.6	17.0	0.90 ± 0.10	18.9
Trp63Ala	5.56 ± 1.5	2.2	0.33 ± 0.04	6.67
Phe140Ala	28.4 ± 3.5	11.2	2.0 ± 0.2	5.60

Table 2: Kinetic constants for Arg 96 and its mutants toward GSH substrate. The units are: V_{max}: μmole/min/mg, K_m: mM, k_{cat}: s-1, k_{cat}/K_m: mM^{-1} s^{-1}. The data are mean + standard deviation from at least 3 independent experiments.

Enzyme	CDNB (1 mM)	DCNB (1 mM)	4-NPB (0.1 mM)	Ethacrynic Acid (0.2mM)
AdGSTD3-3	34.7 ± 2.3	0.0333 ± 0.0149	ND	ND
Arg96Lys	43.5 ± 6.4	0.0321 ± 0.002	ND	ND
Arg96Phe	42.3 ± 9.2	0.0622 ± 0.003	ND	0.0042 ± 0.0019
Arg96Tyr	26.9 ± 4.5	0.0362 ± 0.015	ND	0.0028 ± 0.0007
Arg96Leu	34.0 ± 6.2	0.0264 ± 0.007	ND	<0.006
Arg96Ala	28.3 ± 3.7	0.0233 ± 0.003	ND	<0.001
Arg96Glu	40.3 ± 1.6	0.0711 ± 0.016	ND	<0.15
Pro48Ala	32.7 ± 1.2	0.0412 ± 0.002	ND	0.0093 ± 0.0049
Gln49Ala	47.6 ± 5.6	0.0253 ± 0.011	ND	0.0085 ± 0.0018
Trp63Ala	13.8 ± 0.4	0.0201 ± 0.008	ND	0.0361 ± 0.0061
Phe140Ala	58.1 ± 0.35	0.0774 ± 0.006	ND	<0.012

Table 3: Specific activity of Arg 96 and its mutants towards four different substrates. The units are μmole/min/mg of protein. The data are mean ± standard deviation from at least 3 independent experiments.

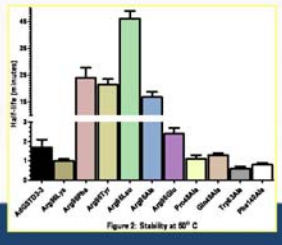

Figure 2: Half-life represents the time of incubation after which 50% activity remains measured in the standard assay system, the conjugation between CDNB (1 mM) and GSH (10 mM)

	0.01 mM BSP	0.1 mM DCNB	0.1 mM 4-NPB Br	0.01 mM Deltamet	0.01 mM Permet	0.001 mM EA	0.01 mM S-hexyl
AdGSTD3-3	71.9±15	15.1 ± 7.4	39.0 ± 7.1	79.1 ± 6.9	81.0 ± 2.3	41.0 ± 8.0	15.6 ± 2.6
Arg96Lys	80.6±2.3	30.4 ± 8.2	57.5 ± 3.1	86.6 ± 0.5	75.8 ± 6.0	55.5 ± 6.1	46.1 ± 2.9
Arg96Phe	58.9±4.8	16.0 ± 4.0	21.7 ± 7.8	37.3 ± 3.3	43.9 ± 9.1	15.3 ± 3.8	22.7 ± 3.5
Arg96Tyr	69.4±8.7	9.6 ± 2.7	27.1 ± 13	62.0 ± 3.5	50.8 ± 4.0	25.4 ± 6.1	25.1 ± 9.9
Arg96Leu	68.7±9.8	23.2 ± 11	28.8 ± 16	54.5 ± 9.0	27.4 ± 8.0	17.5 ± 6.3	17.1 ± 4.9
Arg96Ala	76.0±3.2	36.4 ± 15	46.9 ± 12	89.0 ± 5.3	80.2 ± 5.0	24.4 ± 2.8	34.7 ± 9.5
Arg96Glu	89.3±7.4	31.3 ± 8.5	34.5 ± 5.6	86.9 ± 3.8	68.4 ± 6.8	36.3 ± 3.0	23.3 ± 5.8
Pro48Ala	73.5±2.6	39.0 ± 1.4	46.8 ± 9.3	82.5 ± 7.4	34.8 ± 6.8	37.7 ± 4.9	13.8 ± 10
Gln49Ala	69.7±6.7	9.8 ± 9.2	16.6 ± 10	44.5 ± 6.6	54.7 ± 15	26.9 ± 13	10.6 ± 7.8
Trp63Ala	81.9±5.2	52.8 ± 10	42.5 ± 1.6	57.8 ± 7.5	46.5 ± 5.7	36.1 ± 8.4	7.8 ± 6.3
Phe140Ala	89.6±3.2	59.3 ± 12	56.8 ± 10	81.3 ± 1.5	61.2 ± 8.6	50.4 ± 7.4	41.7 ± 7.4

Table 4: Percent inhibition study of Arg 96 and its mutants from at least three separate experiments. The final concentrations of tested compounds are: 0.01 mM BSP, Bromosulfopthalein; 0.1 mM DCNB, 1,2—dichloro-4-nitrobenzene; 0.1 mM 4-NPB-Br, 4-nitrophenethyl bromide; 0.01 mM deltamethrin, permethrin; 0.001 mM EA, Ethacrynic acid; 0.01 mM S-hexyl glutathione

Conclusion and discussion

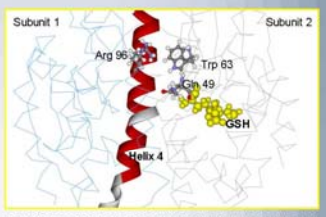

Figure3: Possible mode of communication between Arg96 and Trp63 residues: Backbones are drawn as αcarbon-traces with the exception of the α4 that contains Arg96 of one subunit and the neighboring residues of the alternate subunit. Selected residues are drawn in a ball-and-stick representation, along with Arg96 and nearby interface forming residues. Glutathione is shown as yellow CPK module. The figure was created with DSviewerPro 5.0.

This study shows that mutation of an interface-forming amino acid residue of an insect delta class GST can have an impact on the stability and catalytic function of the enzyme. Arg96 corresponds to Met92 residue in alpha and pi class or Ile92 in mu class GSTs which are the lock residues in those mammalian class GSTs. In addition, Gln49 of AdGSTD3-3 is equal to the Tyr50 or Phe50 of the alpha, mu and pi key residue (Stenberg et al. 2000). Therefore this subunit structure suggests that the mammalian interface may have evolved from the insect ancestor. Arg96 residue not only has a series of residue interactions in the intrasubunit of the protein, it also affects the interaction with Trp63 in the other subunit. Arg96 mutation may affect the rearrangement of Trp63 and indirectly affect Asn47 and Gln49 that are tightly packed in the active site region (Figure 3). For the effect on the stability of the enzyme, Trp63 is located in β 4 that contibutes to stability and folding of GST enzyme in domain 1. The folding in this domain is initiated by interaction between β 2 and β 4 region. Mutation of Trp63 may affect the tertiary structure and thereby reduces the half-life to 50%. This study suggests the role of interface residues of delta class GST may be involved in the stability of the enzyme. The explanation for the modulation of substrate specificity, the V_{max}, and the K_m appears to be due to structural perturbations that induce small changes in active site topology that affect binding and catalysis.

References:
Armstrong RN. Structure, catalytic mechanism, and evolution of the glutathione transferases. Chem Res Toxicol 1997; 10:2-18.
Sheehan D, Meade G, Foley VM, Dowd CA. Structure, function and evolution of glutathione transferases : implications for classification of non-mammalian members of an ancient enzyme superfamily. Biochem J 2001; 360:1-16.
Wongtrakul J, Sramala I, Prapanthadara L and Ketterman A.J. Intra-subunit residue interactions from the protein surface to the active site of Glutathione S-transferase AdGSTD3-3 impact on structure and enzyme properties. Insect. Biochem. Molec. Biol. In press
Stenberg G, Abdalla A-M, Mannervik B. Tyrosine 50 at the subunit interface of dimeric human glutathione transferase P1-1 is a structural key residue for modulating protein stability and catalytic function. Biochem Biophys Res Comm 2000; 271:59-63.

Acknowledgement

This Project was funded to J.W. by the Thailand Research Fund (TRF).

The poster: Interface Residue, Arg 96, Of Glutathione S-transferase Modulates Enzyme Function presented in The Thailand Research Fund annual meeting at Karnchanaburi, 14-16 March 2005